HHS Public Access

Author manuscript

Neuron. Author manuscript; available in PMC 2024 February 15.

Published in final edited form as:

Neuron. 2023 February 15; 111(4): 526–538.e4. doi:10.1016/j.neuron.2022.11.015.

Piezo2 Channels Expressed by Colon-innervating TRPV1-lineage Neurons Mediate Visceral Mechanical Hypersensitivity

Zili Xie[1,6], **Jing Feng**[1,2,6], **Timothy J Hibberd**[3,6], **Bao Nan Chen**[4], **Yonghui Zhao**[1], **Kaikai Zang**[1], **Xueming Hu**[1], **Xingliang Yang**[1], **Lvyi Chen**[1,5], **Simon J Brookes**[4], **Nick J Spencer**[3,*], **Hongzhen Hu**[1,7,*]

[1]Department of Anesthesiology, The Center for the Study of Itch & Sensory Disorders, Washington University School of Medicine, St. Louis, Missouri

[2]Center for Neurological and Psychiatric Research and Drug Discovery, Shanghai Institute of Materia Medica, Chinese Academy of Science, Shanghai, China

[3]Visceral Neurophysiology Laboratory, College of Medicine and Public Health, Flinders University, Adelaide, South Australia, Australia

[4]Neurogastroenterology Laboratory, College of Medicine and Public Health, Flinders University, Adelaide, South Australia, Australia

[5]School of Pharmaceutical Sciences, South-Central University for Nationalities, Wuhan, Hubei, People's Republic of China

[6]These authors contributed equally to this work

[7]Lead contact

Summary

Inflammatory and functional gastrointestinal disorders such as irritable bowel syndrome (IBS) and obstructive bowel disorder (OBD) underlie the most prevalent forms of visceral pain. Although

[*]**Correspondence**: Hongzhen Hu, Center for the Study of Itch and Sensory Disorders, Department of Anesthesiology, Washington University School of Medicine, St. Louis, MO 63110, USA, hongzhen.hu@wustl.edu.; Nick J Spencer, Visceral Neurophysiology Laboratory, College of Medicine and Public Health, Flinders University, Adelaide, South Australia, Australia, nicholas.spencer@flinders.edu.au.

Authors share co-senior authorship

Author contributions

Z.X., J.F., T.J.H., N.J.S., and H.H. conceptualized and participated in the overall design and coordination of the study. Z.X., J.F., T.J.H., B.N.C., Y.Z., K.Z., X.H., X.Y. helped design and execute in vitro and in vivo assays and experiments. T.J.H. and B.N.C. helped with colon nerve recording and VMR recording. Y.Z. helped with RNAscope experiments. K.Z. helped with virus injections. Z.X., J.F., T.J.H., L.C., S.J.B., N.J.S., and H.H. helped with experimental design, execution, and interpretation of the project. Z.X., J.F., T.J.H., S.J.B, N.J.S., and H.H. prepared, wrote, and revised the manuscript.

Declaration of interests

The authors declare no competing interests.

Inclusion and diversity

We support inclusive, diverse, and equitable conduct of research.

Supplemental information

Seven supplement figures were included in the supplemental information.

visceral pain can be generally provoked by mechanical distension/stretch, the mechanisms that underlie visceral mechanosensitivity in colon-innervating visceral afferents remain elusive. Here we show that virally-mediated ablation of colon-innervating TRPV1-expressing nociceptors markedly reduces colorectal distention (CRD)-evoked visceromotor response (VMR) in mice. Selective ablation of the stretch-activated Piezo2 channels from TRPV1 lineage neurons substantially reduces mechanically-evoked visceral afferent action potential firing and CRD-induced VMR under physiological conditions as well as in mouse models of zymosan-induced IBS and partial colon obstruction (PCO). Collectively, our results demonstrate that mechanosensitive Piezo2 channels expressed by TRPV1-lineage nociceptors powerfully contribute to visceral mechanosensitivity and nociception under physiological conditions and visceral hypersensitivity under pathological conditions in mice, uncovering potential therapeutic targets for the treatment of visceral pain.

In brief

Xie et al. show that Piezo2 channels in TRPV1-expressing visceral nociceptors play a major role in visceral pain in mice. Ablation of TRPV1-expressing nociceptors or selective knockout of Piezo2 from TRPV1 lineage neurons reduces colorectal pain under physiological conditions and in mouse models of zymosan-induced IBS and partial colon obstruction.

Keywords

Visceral Mechanosensitivity; Hypersensitivity; Piezo2 Channels; TRPV1-lineage Nociceptors; Irritable Bowel Syndrome; Partial Colon Obstruction

Introduction

Visceral pain is a complaint reported by up to 70% of patients seeking medical care for inflammatory bowel disease (IBD). Moreover, chronic abdominal pain, which lasts for more than three months, is experienced by 20-50% of IBD patients [1]. Visceral pain is also a key feature of functional gastrointestinal (GI) disorders such as irritable bowel syndrome (IBS) and obstructive bowel disorders (OBD). IBS is characterized by pain and altered bowel habits without overt structural changes [2], while OBD is characterized by lumen distention due to mechanical or functional obstruction [3]. OBD is a common clinical problem that may have severe consequences such as pain, sepsis, and perforation, and leads to more than 300,000 admissions in the United States annually [3]. Notably, there is also a high comorbidity of chronic visceral pain with stress-related psychiatric disorders including anxiety, depression, and fatigue [4]. Mechanisms underlying visceral pain are poorly understood and the resulting lack of effective clinical management represents a major unmet medical problem. Remarkably, unlike chronic somatic pain, which is a focus of research and drug development, visceral pain is relatively neglected despite its greater clinical need [5].

Both central and peripheral nervous systems are involved in visceral pain [6]. The gut-brain axis is considered a major factor contributing to motility disorders and visceral hypersensitivity, which may feature dysregulated descending pathways that modulate spinal nociceptive transmission [7]. Emotions and stress can also influence chronic visceral pain

signaling by altering CNS processing [4]. The neural signaling pathway for visceral pain begins with visceral primary afferent neurons of spinal or vagal origin, whose nerve cell bodies reside in the dorsal root ganglia (DRG; spinal) or in the nodose or jugular ganglia (vagal). Their sensory endings reside in the visceral organ and their central axons project into the CNS.

Visceral afferents can be activated and sensitized by tissue injury and inflammation [6]. These conditions can evoke persistent discharge of local nociceptors and subsequent central sensitization, which is essential for transition from acute pain to chronic pain [6]. Ion channels may act as molecular sensors that detect noxious stimuli, which enable nociceptors to encode those stimuli in their action potential firing [8]. Expression of various ion channels in diverse cell types in the GI tract are dynamically regulated in inflammatory and functional GI disorders, and this correlates with pain symptoms [9]. For instance, voltage gated NaV1.5, NaV1.7, and NaV1.9 associate with IBS and visceral hypersensitivity [10]. Mice treated with dextran sodium sulfate (DSS) have significantly increased *Cav3.2* mRNA transcripts compared to untreated animals, and *Cav3.2*-deficient mice are resistant to DSS-induced colonic hypersensitivity [11]. In addition to voltage-gated ion channels, transient receptor potential (TRP) channels, especially TRPV1 and TRPA1, play a significant role in visceral mechanotransduction and inflammation-induced visceral pain [9]. In contrast to their relatively normal somatosensory responses, *Trpv1*-deficient mice show reduced sensitivity to colorectal distension (CRD) compared to congenic C57BL/6J mice [12]. TRPV1, along with acid-sensing ion channel 3 (ASIC3) also mediate visceral hypersensitivity in a mouse model of zymosan-induced IBS [12]. Moreover, administration of TRPV1 and TRPA1 antagonists can prevent the transition from acute to chronic inflammation and pain in a mouse model of chronic pancreatitis [13].

In contrast to the vast array of noxious insults that can activate somatosensory neurons, it is principally mechanical stimulation, such as distension or mesenteric traction, that accounts for most of the painful stimuli in the GI tract [5]. For this reason, there has been great interest in defining the sensory ion channels that enable visceral afferents to detect noxious mechanical stimuli. Among the candidates have been TRP and ASIC channels, which are sensitized by intestinal inflammation and participate in visceral mechanical hypersensitivity, but the role of these ion channels in mammalian mechanotransduction remains unclear [14,15]. Promisingly, recent studies identify Piezo1 and Piezo2 as bona fide mechanically gated ion channels [16]. It is well known that Piezo2 is dominantly expressed in DRG neurons and contributes to innocuous touch sensation under physiological conditions and somatic mechanical allodynia in the setting of tissue inflammation and nerve injury [17,18]. Piezo1 was shown to be selectively expressed in somatostatin (Sst)- and natriuretic polypeptide precursor B (Nppb)-positive pruriceptors and mediates mechanical itch [19]. However, the role of Piezos in visceral mechanotransduction and mechanical hypersensitivity remains elusive. In this study, we show that the mechanosensitive Piezo2 channel, but not Piezo1, expressed by TRPV1-lineage neurons is critically involved in the generation of visceral mechanical nociception under physiological conditions and mechanical hypersensitivity in mouse models of IBS and partial colon obstruction (PCO).

Results

Virally-mediated ablation of colonic TRPV1-expressing nociceptors markedly reduces mechanically evoked visceromotor response

While the somatosensory system combines a mixture of myelinated and unmyelinated fibers for encoding proprioceptive, thermal, nociceptive, and tactile information, the visceral sensory system comprises mainly thin myelinated Aδ and unmyelinated C fibers that are activated primarily by distension/stretch [6]. In the skin, the nociceptive ion channel TRPV1 is also expressed by unmyelinated C fibers and/or thin myelinated Aδ fibers, and ablation of the TRPV1-expressing nociceptors results in complete loss of heat pain sensitivity with little effect on behavioral responses to noxious mechanical or cold stimuli [20]. Interestingly, TRPV1 appears preferentially expressed by visceral afferents compared to somatic afferents [21] and is present in most afferents innervating the urinary and GI tracts [22–24]. To characterize colonic spinal sensory neurons, we first generated TRPV1-tdTomato reporter mice by crossing $Trpv1^{Cre}$ mice [25] with $Ai9^{fl/fl}$ mice [26]. Consistent with a preponderance of TRPV1 expression in visceral afferents, retrograde tracing in $Trpv1^{Cre}$::$Ai9^{fl/fl}$ mice using CTB647 revealed that almost all colon-innervating primary sensory neurons originating from both thoracolumbar (TL; T13 and L1) and lumbosacral (LS; L6 and S1) DRG were TRPV1-tdTomato-positive (Figure S1A). These data, taken together with previous human data indicating that numbers of TRPV1-expressing sensory afferents are increased in rectosigmoid biopsies of IBS patients and correlate with abdominal pain scores [27], suggest TRPV1-expressing sensory afferents may play an important role in visceral mechanical transduction as well as the development of hypersensitivity in mouse colon.

Chemical ablation of TRPV1-expressing nociceptive fibers by resiniferatoxin (RTX) [28,29], an ultrapotent agonist of TRPV1, significantly reduced CRD-induced visceromotor response (VMR) when compared with vehicle-treated mice (Figures S1B and S1C). Consistent with previous findings, systemic TRPV1 neuron ablation markedly reduced somatic heat pain response without affecting mechanical pain (Figures S1D and S1E). Since TRPV1 is broadly expressed by both peripheral and central neurons as well as non-neuronal cells [30], systemic ablation of TRPV1-expressing cells could have potential off-target artifacts. To selectively ablate colon-innervating TRPV1-expressing sensory nociceptors, we injected an AAV9 vector encoding the diphtheria toxin subunit A (DTA) in a Cre-dependent configuration (rAAV-EF1α-DIO-DTA-WPRE-hGH-pA) into the same region of distal colon that was distended by the intraluminal balloon of $Trpv1^{Cre}$ mice ($Trpv1^{AAV\text{-}DTA}$) (Figures 1A and 1B). The rAAV-EF1α-DIO-EGFP-WPRE-hGH-pA virus was used as control virus ($Trpv1^{AAV\text{-}GFP}$). To test the extent of ablation of colon-innervating TRPV1-expressing DRG neurons, retrograde tracer CTB647 was injected into the colon wall at the same sites three weeks later. Consistent with published studies, the results showed that the distal colon is mainly innervated by L6 and S1 DRG neurons (~ 90.2%, 825/915), with a small proportion of DRG neurons were labeled in T13 and L1 DRG neurons (~ 8.5%, 78/915) in control $Trpv1^{AAV\text{-}GFP}$ mice (Figures 1C and 1D). As expected, we found a marked reduction in the number of the CTB647-labeled neurons in $Trpv1^{AAV\text{-}DTA}$ mice when compared with that in $Trpv1^{AAV\text{-}GFP}$ mice (Figure Figures 1C and 1D), suggesting an efficient ablation of the TRPV1-expressing colon-innervating DRG neurons after intracolonic injections of the

DTA virus. Three weeks after virus injections, we further assessed visceral pain responses to graded CRD pressures by recording VMR from the abdominal musculature [31]. There was a marked reduction in the VMR produced by noxious CRD pressures (60 and 80 mmHg) in the Trpv1 $^{AAV\text{-}DTA}$mice when compared to Trpv1$^{AAV\text{-}GFP}$ mice (Figures 1E and 1F). In contrast, the virally-mediated ablation of the colon-innervating TRPV1-expressing DRG neurons did not affect acute somatic mechanical and heat pain (Figures S1F and S1G). These results provide compelling evidence that colon-innervating TRPV1-expressing neurons are a critical component of mechanical transduction and nociception in mouse colon.

Piezo2-expressing colon-innervating TRPV1-lineage neurons contribute to CRD-induced VMR

Merkel disc-expressing Piezo2 channel contributes to the sense of discriminative touch in the steady state[32] while nociceptor-expressing Piezo2 channel mediates somatic mechanical allodynia in the setting of inflammation or nerve injury [17,18]. In the viscera, Piezo2 in urothelial cells serves as a mechanosensor in the urinary bladder to coordinate voiding and mediates urothelial mechanotransduction and lower urinary tract interoception [33,34]. Thus, the next question addressed was whether Piezo2 also contributes to visceral mechanosensitivity in the GI tract and if so, by what mechanisms does this occur.

By using single-cell quantitative reverse transcription polymerase chain reaction (qRT-PCR) analysis on retrogradely traced colon-innervating LS DRG neurons from wild type C57BL/6J mice, *Piezo*2 mRNA transcripts were detected in 53.6% (15 of 28) of CTB488-labeled DRG neurons (Figure 2A). TRPV1 mRNA transcripts were detected in 89.3% (25 of 28) of CTB488-labeled DRG neurons, with 56.0% (14 of 25) of the TRPV1-positive neurons also expressed *Piezo2* mRNA transcripts (Figure 2A). Strikingly, 93.3% (14 of 15) of the *Piezo2*-positive CTB488-labeled DRG neurons expressed *Trpv1* mRNA transcripts. The extensive overlapped expression of *Piezo2* with *Trpv1* suggests that Piezo2 expressed by the TRPV1-expressing visceral nociceptors may play a critical role in visceral mechanosensitivity and nociception. We therefore generated nociceptor-specific *Piezo2* conditional knockout mice in which Piezo2 function was selectively ablated from TRPV1-lineage nociceptors by crossing Trpv1^{Cre} mice with Piezo2$^{fl/fl}$ mice. Using RNAscope *in situ* hybridization we detected a marked reduction of *Piezo2* mRNA transcripts in CTB488-labeled LS DRG neurons retrogradely traced from the colon of the Trpv1^{Cre}::Piezo2$^{fl/fl}$ mice when compared with that from the Piezo2$^{fl/fl}$ control littermates (Figure 2B). Next, in CTB488-labeled LS DRG neurons, we recorded whole-cell mechanically activated (MA) currents evoked by mechanical indentation using a piezoelectrically actuated blunt glass probe [16]. Based on inactivation kinetics, whole-cell MA currents can be further classified as rapidly adapting (RA), intermediately adapting (IA), and slowly adapting (SA) [16]. Surprisingly, almost all mechanically activated colon-innervating LS DRG neurons displayed Piezo2-like RA current in response to mechanical indentation in Piezo2$^{fl/fl}$ control mice (Figure 2C). Importantly, the proportion of mechanosensitive DRG neurons, as well as the maximal MA current density, was significantly reduced in CTB488-labeled DRG neurons isolated from Trpv1^{Cre}::Piezo2$^{fl/fl}$ mice when compared with those from Piezo2$^{fl/fl}$ control mice (Figures 2C–2E), consistent with loss of Piezo2 function in colon-innervating

LS DRG neurons in the Trpv1^{Cre}::Piezo2$^{fl/fl}$ mice. A small proportion of LS DRG neurons showing MA current (9.8%; 5 of 51) remained in Trpv1^{Cre}::Piezo2$^{fl/fl}$ mice. We speculate these neurons may represent Piezo2-expressing TRPV1 negative neurons, and/or Piezo1-expressing neurons, which has been recently identified in DRG neurons mediating itch sensation [19].

To further examine the role of Piezo2 in colon-innervating sensory afferents, sensitivity to circumferential stretch was tested in *ex vivo* visceral afferent recordings from both Piezo2$^{fl/fl}$ and Trpv1^{Cre}::Piezo2$^{fl/fl}$ colon preparations. As expected, circumferential stretch evoked colonic afferent action potential firing in a force-dependent manner (Figures 2F and 2G). Strikingly, stretch-evoked action potential firing was significantly reduced in Trpv1^{Cre}::Piezo2$^{fl/fl}$ mice when compared to Piezo2$^{fl/fl}$ control littermates (Figures 2F and 2G). To further test the possibility that Piezo2 mediates other types of mechanical stimuli in the colon, we applied focal mechanical probing and mucosal brushing to the colon preps. Not surprisingly, action potential firing induced by both probing and brushing was also significantly reduced in Trpv1^{Cre}::Piezo2$^{fl/fl}$ mice (Figure S2). Consistent with *ex vivo* visceral afferent recordings, the CRD-induced VMR was also significantly attenuated in the Trpv1^{Cre}::Piezo2$^{fl/fl}$ mice compared to Piezo2$^{fl/fl}$ control mice at 40, 60, and 80 mmHg CRD pressures (Figures 2H and 2I). Taken together, these results demonstrate that Piezo2 channels expressed by the TRPV1-lineage neurons are sensitive to various types of mechanical stimuli and mediate mechanical force-evoked colonic afferent firing, thus play an important role in visceral mechanotransduction and nociception under physiological conditions.

Virally-mediated ablation of Piezo2 function from the colon-innervating DRG neurons markedly suppresses CRD-evoked VMR

The conditional knockout approach causes ablation of Piezo2 channel function from all TRPV1-lineage DRG and trigeminal neurons. To restrict this genetic manipulation to colonic visceral afferents, we injected AAV9 vectors encoding a GFP-Cre (pENN.AAV.hSyn.HI.eGFP-Cre.WPRE.SV40) virus or GFP (AAV-hSyn-EGFP) control virus into the colon wall of Piezo2$^{fl/fl}$ mice (Figure 3A). Three weeks after virus injections, whole-cell MA currents were recorded from GFP-labeled LS DRG neurons. About 36.6% of the colon-innervating LS DRG neurons isolated from Piezo2$^{AAV\text{-}GFP}$ control mice showed MA currents (Figures 3B–3D). The colon-innervating LS DRG neurons isolated from Piezo2$^{AAV\text{-}GFP\text{-}Cre}$ mice displayed a marked reduction in both the proportion of mechanically sensitive DRG neurons and their maximal MA current density, suggesting that Piezo2 is required for MA currents in colon-innervating LS DRG neurons (Figures 3B–3D).

We next tested whether Piezo2 expression in colon-innervating DRG neurons is required for CRD-evoked visceral mechanosensitivity. Indeed, VMRs evoked by CRD pressures at 60 mmHg and 80 mmHg were significantly diminished in Piezo2$^{AAV\text{-}GFP\text{-}Cre}$ mice compared to Piezo2$^{AAV\text{-}GFP}$ mice (Figures 3E and 3F). These findings demonstrate that Piezo2 expressed by the colon-innervating LS DRG neurons mediates a substantial component of the CRD-induced VMR. In marked contrast, the acute heat and mechanical pain responses in the skin were indistinguishable between the Piezo2$^{AAV\text{-}GFP\text{-}Cre}$ and Piezo2$^{AAV\text{-}GFP}$ mice,

confirming the specificity of Piezo2 ablation to colonic visceral afferents (Figure S3A to S3C). Moreover, although Piezo1 channel is reported to be expressed by DRG neurons [35,36], the CRD-induced VMR was comparable between the Piezo1$^{AAV\text{-}GFP\text{-}Cre}$ and Piezo1$^{AAV\text{-}GFP}$ mice (Figure S4A to S4C), suggesting that Piezo1 is either not functionally expressed by colonic DRG neurons as reported [32] or Piezo1-expressing colon-innervating visceral sensory nociceptors contribute little to CRD-induced visceral mechanosensitivity under physiological conditions.

Piezo2 mediates visceral mechanical hypersensitivity in a mouse model of IBS

Zymosan, derived from the cell wall of yeast, is widely used to induce visceral hypersensitivity, comparable to patients with IBS [37]. Application of zymosan neither changed colonic structure nor induced neutrophil-related colonic inflammation (Figures 4A–4C) although colonic mast cell and macrophage infiltration has been observed in zymosan-treated mice [38,39]. To test if Piezo2 contributes to zymosan-induced visceral hypersensitivity, we first investigated Piezo2 function in retrogradely labeled colon-innervating LS DRG neurons isolated from the zymosan-treated mice. Overall, 44.7% of the CTB488-labeled colon-innervating DRG neurons responded to mechanical indentation in zymosan-treated C57BL/6J mice, while only 30.2% were activated in vehicle-treated C57BL/6J mice (Figures 4D and 4E). The maximal current density of the Piezo2-like whole-cell MA currents was also significantly increased in the CTB488-labeled colon-innervating DRG neurons isolated from the zymosan-treated C57BL/6J mice compared to those from vehicle-treated C57BL/6J mice (Figure 4F). To investigate whether the expression of Piezo2 is increased after zymosan treatment, we did RT-PCR using L6 and S1 DRGs. The results showed that the expression of Piezo2 is significantly increased in the DRG neurons isolated from zymosan-treated mice compared to those from vehicle-treated mice (Figure 4G). *Ex vivo* colonic afferent recordings showed that circumferential stretch-evoked firing was significantly increased in zymosan-treated Piezo2$^{fl/fl}$ mice but not in zymosan-treated Trpv1^{Cre}::Piezo2$^{fl/fl}$ mice (Figures 4H, 4I and S5A). Consistent with afferent nerve recordings, CRD-enhanced VMR in Trpv1^{Cre}::Piezo2$^{fl/fl}$ mice was also markedly reduced compared with Piezo2$^{fl/fl}$ control littermates subjected to zymosan treatment (Figures 4J, 4K, S5B, and S5C). These findings suggest that the contribution of Piezo2 is increased by zymosan treatment, causing hypersensitivity to CRD.

Piezo2 mediates visceral mechanical hypersensitivity in a mouse model of PCO

PCO is a common clinical problem associated with severe pain, sepsis, and perforation [40]. Experimental PCO in mice causes abnormal morphological changes and hyperexcitability of primary sensory neurons, which may underlie enhanced visceral pain behavior [41]. Because bowel obstruction is accompanied by lumen distention, we speculated that Piezo2 may transduce mechanical stimulation and mediate visceral hypersensitivity provoked by PCO. Consistent with previous studies, mice subjected to PCO procedure had a significantly increased colon diameter accompanied by increased immune infiltration as shown by markedly increased number of MPO-positive neutrophils (Figures 5A to 5C). No significant differences in PCO-induced inflammation were observed between the Piezo2$^{fl/fl}$ and Trpv1^{Cre}::Piezo2$^{fl/fl}$ mice, suggesting that nociceptor-expressed Piezo2 channel function is probably not involved in the inflammatory response produced by PCO (data not shown).

We next tested if Piezo2 function was affected in CTB488-labeled colon-innervating DRG neurons isolated from PCO-treated mice (Figure 5D). The proportion of CTB488-labeled colon-innervating LS DRG neurons activated by mechanical indentation was 54.3% in PCO mice, compared to 36.6% in sham-treated mice (Figure 5E). The maximal current density of Piezo2-like RA currents was also significantly increased in CTB488-labeled colon-innervating LS DRG neurons isolated from PCO mice, compared with those from sham treated mice (Figures 5D to 5F). The expression of Piezo2 was also significantly increased in LS DRG neurons isolated from PCO mice, compared with those from sham control mice (Figure 5G). Moreover, while PCO enhanced stretch-induced firing in visceral afferents, this enhancement was substantially reduced in $Trpv1^{Cre}$::$Piezo2^{fl/fl}$ mice compared to $Piezo2^{fl/fl}$ control littermates (Figures 5H, 5I and S5D). Likewise, PCO enhanced VMRs evoked by colonic distension and this enhancement was greatly reduced in $Trpv1^{Cre}$::$Piezo2^{fl/fl}$ mice compared to $Piezo2^{fl/fl}$ control littermates (Figures 5J, 5K, S5E, and S5F). Taken together, these results show Piezo2 in TRPV1-lineage neurons significantly contributes to PCO-enhanced visceral mechanical hypersensitivity.

Consistent with the data from our genetic manipulation of Piezo2 functions in the conditional knockout mice, virally mediated knockdown of Piezo2 function from the colon-innervating DRG neurons also displayed reduced visceral hypersensitivity in both zymosan model and PCO models (Figure 6). Moreover, blocking Piezo2 with acute intraperitoneal injection of GsMTx4 could also alleviate CRD-induced visceral nociception under normal condition and visceral hypersensitivity caused by zymosan and PCO (Figure S6).

Immobility (reduced voluntary movements) is commonly used as a proxy measurement for spontaneous pain in both somatic and visceral models [42–44]. We measured voluntary movement to quantify spontaneous pain behaviors in mice subjected to treatment with either zymosan or PCO. Surprisingly, zymosan-treated mice did not show differences in total traveling distance, time spent stationary, or time spent moving when compared with vehicle-treated mice. This suggests that zymosan induces IBS-like inflammatory visceral hypersensitivity which is insufficient to produce spontaneous visceral pain without exogenous distension (Figure S7A to S7E). In marked contrast, the total traveling distance and time spent moving were significantly decreased after PCO treatment, while the time spent stationary was significantly increased (compared with sham treatment) (Figures 7A–7E). This effect was partially reversed by ibuprofen, a nonsteroidal anti-inflammatory drug used to treat pain, including visceral pain (Figure S7F–7H) [45]. This suggests PCO drives spontaneous visceral pain behaviors in mice. Importantly, the decreased distance moved, time spent moving and the increased time spent stationary after PCO treatment were all significantly reduced in $Trpv1^{Cre}$::$Piezo2^{fl/fl}$ mice, compared to $Piezo2^{fl/fl}$ control littermates (Figures 7F–7I). This suggests that Piezo2 contributes to the generation of spontaneous (non-evoked) visceral pain in PCO mice.

Discussion

Nociceptive TRP channels, especially TRPV1 and TRPA1, play a critical role in neurogenic inflammation and pain [46]. TRPV1 and TRPA1 are also important mediators of visceral hypersensitivity [46] and pharmacological inhibition of TRPV1 and TRPA1 reduces visceral

hypersensitivity in various animal models of colonic inflammation [47]. Therefore, TRPV1 and TRPA1 have been considered as potential therapeutic targets for treatment of colitis and visceral hypersensitivity [46]. The results of this study support the importance of TRPV1-expressing nociceptors as a key mediator of both somatic and visceral pain. Our results further support the involvement of the TRPV1-expressing visceral afferents in visceral mechanosensitivity and nociception since selective ablation of colon-innervating TRPV1-expressing visceral nociceptors using a viral Cre-loxp approach mitigated stretch-evoked *ex vivo* visceral afferent firing and *in vivo* CRD-induced VMR. More importantly, selective ablation of Piezo2 function from TRPV1-lineage neurons also reduced stretch-evoked visceral afferent firing and CRD-induced VMR.

Consistent with our findings, a recent study showed that chemogenetic inhibition of TRPV1-expressing visceral nociceptors using Gi-DREADD (Designer Receptors Exclusively Activated by Designer Drugs) attenuated visceral hypersensitivity in a mouse model of chemical-induced colitis [48]. Moreover, optogenetic stimulation of visceral afferents in TRPV1-ChR2 (channelrhodopsin-2) mice evoked action potential firing in 86% of the fibers recorded;57% of those responsive fibers were stretch-sensitive [49].

Our *in vitro* and *in vivo* experiments show that Piezo2 is functionally expressed in TRPV1-lineage neurons most of which have previously been shown to co-express TRPV1 and TRPA1 [50,51]. Our results showed that 93.3% of the *Piezo2*-positive colonic DRG neurons also expressed *Trpv1* mRNA transcripts. These results are consistent with Hockley's single cell RNAseq data [52]. However, Meerschaert's study showed a lower percentage of overlap between *Piezo2* and *Trpv1* in colonic DRG neurons. In their study, only 78.05% of LS DRG neurons showed detectable expression of *Trpv1*. Of note, this data conflicts with their calcium imaging results, in which capsaicin activates 95.45% of LS DRG neurons [53].

Our findings suggest that Piezo2 channels, expressed by TRPV1-lineage neurons, are involved in visceral mechanical hypersensitivity. Previous studies have demonstrated a role for TRPA1/TRPV1 in visceral hypersensitivity [47]. From this we speculate that TRPV1-lineage neurons regulate chemosensory responses through sensitization of TRPA1/TRPV1 channels and regulate mechanosensory mechanisms via sensitization of Piezo2. However, Piezol channels are unlikely to be involved. These combined mechanisms drive action potential firing in visceral nociceptors, promoting mechanical hypersensitivity associated with intestinal inflammation and tissue injury. Intriguingly, Borbiro et al. showed that capsaicin-induced activation of TRPV1 inhibits Piezo2 channel function through depletion of phosphoinositides [54]. Other studies demonstrated reciprocal regulation of TRPV1 and TRPA1 [55–57]. In addition to TRP channels, previous studies showed that Cav3.2 channels are involved in the pathogenesis of visceral pain [58–61]. Since Piezo2 activation by mechanical stimulation promotes visceral nociceptor excitability, Cav3.2 likely serves as a mediator of visceral pain downstream of Piezo2-mediated action potential firing. Therefore, interaction and integration of functions of various ion channels including Piezo2, Cav3.2, and TRPV1 likely shape the duration and intensity of mechanically activated visceral nociception and hypersensitivity. In combination, these studies show a capacity for complex regulation of multiple nociceptive ion channels in the TRPV1-lineage neurons in visceral mechanical hypersensitivity.

It is well-established that loss of Piezo2 function in Merkel cells and primary sensory neurons causes insensitivity to discriminative touch in mice. Loss-of-function mutations in humans cause profound deficits in discriminative touch perception and proprioception [32,62]. On the other hand, Piezo2-deficient neurons still respond robustly to noxious pinch [18] and individuals with loss-of-function Piezo2 mutations can still sense deep tissue pressure similar to healthy control subjects [63]. They also maintain the ability to detect acute mechanical pain [64]. These studies suggest that Piezo2 is not a mechanosensor for acute noxious somatic mechanical stimuli. Surprisingly, our study clearly demonstrated that the VMR induced by noxious intraluminal colonic distension pressures at 60 and 80 mmHg was markedly reduced in mice with selective ablation of Piezo2 function in colon-innervating visceral nociceptors. This suggests that the stretch-activated Piezo2 channel plays a major role in sensing noxious mechanical forces in visceral sensory neurons but not in somatic sensory nociceptors. We speculate that this explains why the visceral sensory system is primarily activated by distension/stretch.

Piezo2 deficiency in primary nociceptors reduces somatic mechanical allodynia to both capsaicin-induced inflammation and in spared nerve injury in mice [17]. Strikingly, individuals with loss-of-function mutations in Piezo2 do not develop mechanical allodynia after skin inflammation [18]. This is compelling evidence that Piezo2 mediates inflammation- and nerve injury-induced cutaneous mechanical allodynia in mice and humans. The present study showed that Piezo2 function is required for visceral mechanical hypersensitivity in mouse models of PCO and zymosan-induced IBS. Taken together, these findings suggest that Piezo2 contributes to both somatic and visceral mechanical hypersensitivity following tissue inflammation and injury. Many studies showed the important roles of immune cells as well as glia in visceral pain [65,66]. Although the underlying mechanism remains unclear, we speculate that visceral hypersensitivity might be partially caused by increased expression of Piezo2. On the other hand, increased levels of inflammatory mediators released from immune cells in the inflamed or injured tissues may sensitize Piezo2 function, leading to enhanced mechanical sensitivity. Indeed, PIEZO2-mediated MA currents are enhanced 8-fold by bradykinin in DRG neurons [67]. Moreover, extracellular ATP and NGF are also potent Piezo2 sensitizers [68,69]. NGF also sensitizes the nicotinic acetylcholine receptor subunit alpha-3 (CHRNA3)-expressing “silent nociceptors”, which is mediated by Piezo2 [70]. Intracellular signaling pathways involving cAMP, EPAC1, Gβγ, PKA, and PKC have all been reported to cause Piezo2 sensitization [67–69,71,72]. Future studies are needed to determine which of these signaling molecules is involved in PIEZO2-mediated visceral mechanical hypersensitivity in the setting of GI inflammation and obstruction.

In summary, our results demonstrate that Piezo2 channels expressed by TRPV1-lineage visceral nociceptors mediate a large component of acute visceral mechanical nociception under physiological conditions. Importantly, Piezo2 channels expressed by TRPV1-lineage visceral nociceptors also emerged as a critical mediator of pathologic visceral mechanical hypersensitivity in mouse models of IBS and PCO, thus identifying Piezo2 channel as a potential therapeutic target for the treatment of chronic visceral pain.

STAR Methods

Resource availability

Lead contact—Further information and requests for resources and reagents should be directed to and will be fulfilled by the lead contact, Hongzhen Hu (hongzhen.hu@wustl.edu).

Materials availability—This study did not generate new unique reagents.

Data and code availability—Data reported in this paper are available from the lead contact upon reasonable request.

This paper does not report original codes.

Any additional information required to reanalyze the data reported in this paper is available from the lead contact upon request.

Experimental model and subject details

Transgenic mice—All animal experiments used in this study were approved by the Animal Studies Committee at Washington University in Saint Louis School of Medicine and were done in accordance with the guidelines of the National Institutes of Health and the International Association for the Study of Pain. Wild-type C57BL/6J, Ai9$^{fl/fl}$, Piezo1$^{fl/fl}$, and Piezo2$^{fl/fl}$ were obtained from the Jackson Laboratory (Bar Harbor, ME, USA). Trpv1^{Cre} mice were donated by Dr. Mark Hoon from NIH. Mice were housed under a standard 12:12 hour light-dark condition with free access to water and food. Mice facility core staff and researcher monitored mice daily. Mice were used in behavior experiments at about 8 weeks of age. 3-weeks old mice were used for virus injection. All behavioral tests were done by observers blind to the genotypes of mice. Experiments were performed on independent cohorts of male and female mice and no differences between the sexes were found. For all experiments, the number of replicates and statistical test used are reported in figure legends. The reported replicates refer to biological replicates. Sample sizes were within the range generally used in the visceral pain field. Data were not excluded in any studies.

Method details

Intracolonic injections—Mice were anesthetized with 3% isoflurane followed by 1% isoflurane to maintain anesthesia. To prevent dehydration of eyes, artificial tears were used. After shaving and sterilization of the abdomen, mice were placed on a sterile surgical pad and covered with a sterile surgical drape. The colon was exposed by making a midline incision through the abdominal wall. 2 μL of CTB or virus (500 nL*4 sites) was injected at a flow rate of 100 nL/minute to enhance convection with a pulled glass pipette, and the needle was left in place for at least 5 minutes to prevent reflux. Following injection, the abdominal wall was sutured, and skin was closed using surgical sutures. Antibiotic ointment was applied to the closed surgical site. Tissues were collected for analysis 5 days after CTB injections. Behavioral data and tissues were collected for analysis 3 weeks after AAV injections.

Electrode implant for VMR—Mice were anesthetized with inhaled 3% isoflurane for induction, reduced to 1% for maintained anesthesia. The hair of the lower right abdominal area and the back of the neck was removed with a clipper and the shaved areas were disinfected with betadine. A small (about 1 cm) incision was made in the skin of the lower right abdomen. Small scissors were used to separate the skin from the abdominal musculature around the incision. A small incision (about 0.5 cm) was then made in the skin overlying the back of the neck. A sterile glass tube (about 1.5 mm diameter) was then subcutaneously tunneled from the neck incision to the abdominal incision. Two sterilized and insulated stainless steel EMG electrode wires (about 10 cm length; FE632111, Advent Research Materials, Oxford, England) were threaded through the glass tube. The glass tube was removed, the electrodes tips (2 – 3 mm) were exposed by removing the insulation and then secured in the abdominal musculature with suture. The skin was closed using sutures.

CRD-induced VMR—The CRD-system was composed of a Distender Series II barostat (G and J Electronics, Toronto, ON, Canada) and an amplifier for electrophysiological recordings from the abdominal electrodes (ISO-80, World Precision Instruments, Sarasota, FL). A custom-made balloon (1 cm length x 1 cm inflated diameter) prepared from a condom was tied over a PE60 catheter with silk 4.0. On the experimental day, mice were lightly anesthetized with 2% isoflurane and a lubricated balloon with a connecting catheter was inserted into the colon 2 cm proximal to the anus. The catheter was fixed to the base of the tail with tape to avoid any displacement. Mice were restrained using a 50 ml plastic tube and were allowed to recover for 30 min before colorectal distension. The balloon was connected to the barostat system and was distended with barostat equipment under computer control using ProtocolPlus Deluxe and Labchart softwares. The ascending phasic distension (from 10 to 80 mmHg) paradigm, consisting of three 10 s pulses at each pressure and at least 5-min inter-pulse intervals, was used. The visceromotor responses (VMR) were quantified as pressure changes in the colonic distending balloon during the colorectal distension procedure. VMR were calculated as the average of the three pulses for each pressure.

Treatment of RTX to ablate TRPV1-expressing nociceptive fibers—4-week-old mice were subcutaneously injected with RTX (Sigma, St. Louis, MO) into the flank in three escalating (30, 70, and 100 μg/kg) doses on consecutive days. Control mice were injected with vehicle solution. RTX- or vehicle-treated mice were allowed to rest for at least 4 weeks before behavioral test.

Zymosan-induced IBS model—At day 0, baseline response of VMR to CRD (1^{st} VMR) was measured and mice were then anesthetized with 2 % isoflurane inhalation and the distal colon was carefully rinsed with 1ml of saline via intrarectal perfusion at a distance of 2 cm from the anus via a 18-gauge, 5-cm-long disposable feeding needle, followed by the intrarectal application of 1 ml of 30% ethanol to remove the mucous barrier and another 1 ml saline to rinse the colon. Zymosan and saline were given daily for three consecutive days from day 1 to day 3. Briefly, 0.1 ml of zymosan (a Glucan prepared from yeast cell wall characterized as a protein-carbohydrate complex, Sigma, St. Louis, MO) suspension of 30 mg/ml in saline was injected into the colons of mice over a period of 5 min via a feeding

needle. Control mice were injected with 0.1 ml of saline. Response of VMR to CRD (2^{nd} VMR) was measured on day 4. Visceral hypersensitivity induced by zymosan was assessed using the formula of ΔVMR=2^{nd} VMR-1^{st} VMR.

Mouse model of PCO—At day 0, baseline response of VMR to CRD (1^{st} VMR) was measured before assessing colorectal hypersensitivity. At the same day, mice were anesthetized using 2% isoflurane inhalation. After midline laparotomy, a distal colon segment 3 cm proximal to the end of colon was carefully exposed. A customized 3-mm diameter medical grade silicon ring was mounted around the colon wall. The sham control mice underwent the same surgical procedure except that the ring was removed immediately after the procedure. The skin was closed using sutures. At day 4, response of VMR to CRD (2^{nd} VMR) was measured and visceral hypersensitivity induced by PCO was assessed using the formula of ΔVMR=2^{nd} VMR-1^{st} VMR.

Open field test—To determine spontaneous pain-like behaviors in zymosan-treated mice and PCO mice, the open field (OF) test was carried out. The mouse was placed in the center of a square arena (25 cm × 25 cm × 30 cm) and acclimated for 10 min. The horizontal locomotor activity of the mice within 5 min was videotaped and analyzed with EthoVision XT software to measure travel distance, time spent moving and time spent stationary.

Virus—pENN.AAV.hSyn.HI.eGFP-Cre.WPRE.SV40 was a gift from James M. Wilson (Addgene viral prep # 105540-AAV9; http://n2t.net/addgene:105540 ; RRID:Addgene_105540). pAAV-hSyn-EGFP was a gift from Bryan Roth (Addgene viral prep # 50465-AAV9; http://n2t.net/addgene:50465 ; RRID:Addgene_50465). rAAV-EF1α-DIO-DTA-WPRE-hGH-pA (BrainVTA, PT-0345) and rAAV-EF1α-DIO-EGFP-WPRE-hGH-pA (BrainVTA, PT-0795) were purchased from BrainVTA.

Isolation and culture of DRG neurons—Briefly, laminectomies were done before DRG (L6 and S1) were dissected out. After removal of connective tissues, DRG were placed in 1 mL Ca^{2+}/Mg^{2+}-free Hank's Balanced Salt Solution (HBSS) containing 2 mg collagenase type II (Worthington Biochemical, Lakewood, NJ, USA) and 2 mg dispase (Worthington Biochemical) for 45 min. Neurons were gently triturated, pelleted, and then re-suspended in Neurobasal-A culture medium containing 1% B-27 supplement (ThermoFisher Scientific, Waltham, MA, USA), 100 U/mL penicillin plus 100 μg/mL streptomycin (Sigma-Aldrich, St. Louis, MO, USA), 100 ng/mL nerve growth factor (NGF, Sigma), 20 μg/mL glial cell-derived neurotrophic factor (GDNF, Sigma-Aldrich) and 10% heat-inactivated FBS (Sigma-Aldrich). After plating, DRG neurons were cultured in a humidified incubator at 37 °C for at least 24 h before use.

Single DRG neuron picking—DRG neurons were dissociated and purified using a 15% BSA density gradient column. GFP- or CTB488-labeled neurons were visually identified under a Nikon Eclipse TE200-S microscope (Tokyo, Japan) and manually picked using a micromanipulator (Sutter Instrument, Novato, CA). Pre-sterilized glass electrodes filled with HBSS were used to harvest individual DRG neurons. The single isolated DRG neuron was drawn into the tip of a glass electrode by applying negative pressure and was transferred to a PCR tube containing 10 μL of Single Cell Lysis/Dnase I solution (4458237, Invitrogen).

The contents were incubated at room temperature for 5 min, then 1 μL of Stop Solution was added to lysis reaction. The samples were stored at −20 °C until cDNA synthesis.

Single cell RT-PCR—Single cell RT-PCR were performed with Invitrogen Single Cell-to-CT™ Kit (4458237, Invitrogen) according to the manufacturer's manual. The primers of *Piezo2*, *Trpv1*, *Gfap*, and *Gapdh* were mixed with preamplification reaction mix and 2 μL of the products from the preamplification was used for the real-time RT-PCT reaction.

Whole-Cell Patch-clamp recordings—Whole-Cell Patch-clamp recordings were performed at room temperature using an Axopatch 200B amplifier (Axon Instruments). The resistance of patch pipette was 3–4 MΩ when filled with an internal solution consisting of (in mM): 133 CsCl, 10 HEPES, 5 EGTA, 1 $CaCl_2$, 1 $MgCl_2$, 4 MgATP, and 0.4 Na_2GTP (pH adjusted to 7.3 with CsOH). The extracellular solution was made of (in mM): 127 NaCl, 3 KCl, 1 $MgCl_2$, 10 HEPES, 2.5 $CaCl_2$, 10 glucose (pH adjusted to 7.3 with NaOH). Currents were sampled at 20 kHz and filtered at 2 kHz. Leak currents before mechanical stimulations were subtracted off-line from the current traces. Mechanical stimulation was achieved using a fire-polished glass pipette (tip diameter 3–4 μm) positioned at an angle of 85° to the cell being recorded. The probe was advanced onto the cell by a Clampex controlled piezo-electric crystal microstage (E625 LVPZT Controller/Amplifier; Physik Instrumente). To measure the maximal current density evoked by mechanical stimuli, a series of steps in 1 μm increments were applied every 10 s, which allowed full recovery from mechanical stimulation. Inward MA currents were recorded at a holding voltage of −80 mV.

***Ex vivo* afferent recording from colorectum-pelvic nerve preparations—**Mice were sacrificed and ~3 cm of distal colorectum was removed along with the pelvic/rectal nerves. Tissues were placed into ice-cold Krebs' solution bubbled with carbogen and then transferred to an organ bath consisting of two adjacent chambers separated by a plastic gate. The colon was opened longitudinally along the mesenteric border and the full thickness preparation was placed in a Sylgard-lined chamber with circulating Krebs' solution maintained at 35°C and pinned flat with mucosal side up. Multiple rectal nerves leading to the pelvic ganglia were dissected free of surrounding connective tissue. The nerves were then pulled into a chamber filled with mineral oil and placed on a mirror plate. Small bundles of the nerve were teased and hung on a gold electrode for action potential recordings. Signals were amplified (ISO80; WPI, Sarasota, FL, USA) and recorded at 20 kHz (PowerLab16sp, LabChart 7, ADInstruments, Castle Hill, NSW, Australia). A calibrated isotonic transducer (Harvard Bioscience, model 52-9511, S. Natick, MA, USA) was coupled to preparations via a pulley and an array of hooks, 5-10 mm wide. Distending loads used to stretch the gut in the circumferential axis were applied as weights attached to the arm of the isotonic transducer. Distensions were held for a duration of 10 seconds, with a recovery period of 5 minutes between distensions. Focal mechanical probing and mucosal brushing were applied according to published paper [73].

Histology—Mice were anesthetized using ketamine–xylazine cocktail and transcardially perfused with 30 ml of ice-cold PBS followed by 30 ml of ice-cold 4% paraformaldehyde (PFA). DRG and colon tissues were dissected and were post-fixed in ice-cold PFA for

overnight. Tissues were cryoprotected in 30% (wt/vol) sucrose–PBS solution for 48 h before they were frozen in OCT. Tissues were sectioned at 12 μm with a Leica CM-1950 cryostat, allowed to air dry for 30 min and washed using PBS containing 0.3% Triton-X 100 (PBST). Tissue sections carrying endogenous fluorescence were directly mounted using Fluoromount-G. Tissue sections that required staining were blocked using 10% normal goat serum for 1 h at room temperature and incubated in primary antibody at 4 °C overnight. Tissues were washed three times for 10 min each time and were stained with secondary antibody at room temperature for 3 h. After staining, tissue sections were mounted using Fluoromount-G and imaged using a Nikon C2 confocal microscope with NIS-Elements imaging software (Nikon Instruments Inc., Melville, NY, USA).

Quantification and statistical analysis—All retrograde tracing, patch-clamp, histology, and *ex vivo* afferent recording experiments were repeated using cells or tissues from at least three different mice. All attempts at replication were successful. Sample sizes for VMR recording and open field test were selected on the basis of power analysis of related publications. Statistical analysis was performed using GraphPad Prism 7.0 (GraphPad). Unless stated otherwise, data are presented as mean ± s.e.m. for n independent observations. Variable differences between two experimental groups were assessed using two tailed unpaired Student's *t* test, as indicated in figure legends. Two-way Analysis Of Variance (ANOVA) with Bonferroni *post-hoc* analysis was used for comparisons of multiple treatment groups. P values were used to determine statistical significance and $P<0.05$ was considered significant.

Supplementary Material

Refer to Web version on PubMed Central for supplementary material.

Acknowledgments

We thank our lab members and colleagues for critical reading of this manuscript. This project was supported by grants from National Institutes of Health grant R01AA027065 (NINDS, H.H.), National Institutes of Health grant R01AR077183 (NIAMS, H.H.) and National Institutes of Health grant R01DK103901 (NIDDK, H.H.). N.J.S. acknowledges NHMRC grant 1156416 to support T.J.H.

References:

1. Zielinska A, Salaga M, Wlodarczyk M, and Fichna J (2019). Focus on current and future management possibilities in inflammatory bowel disease-related chronic pain. Int J Colorectal Dis 34, 217–227. 10.1007/s00384-018-3218-0. [PubMed: 30564910]
2. Al-Chaer ED, Kawasaki M, and Pasricha PJ (2000). A new model of chronic visceral hypersensitivity in adult rats induced by colon irritation during postnatal development. Gastroenterology 119, 1276–1285. 10.1053/gast.2000.19576. [PubMed: 11054385]
3. Shi XZ, Lin YM, and Hegde S (2018). Novel Insights Into the Mechanisms of Abdominal Pain in Obstructive Bowel Disorders. Front Integr Neurosci 12, 23. 10.3389/fnint.2018.00023. [PubMed: 29937720]
4. Greenwood-Van Meerveld B, and Johnson AC (2017). Stress-Induced Chronic Visceral Pain of Gastrointestinal Origin. Front Syst Neurosci 11, 86. 10.3389/fnsys.2017.00086. [PubMed: 29213232]
5. Gebhart GF, and Bielefeldt K (2016). Physiology of Visceral Pain. Compr Physiol 6, 1609–1633. 10.1002/cphy.c150049. [PubMed: 27783853]

6. Sengupta JN (2009). Visceral pain: the neurophysiological mechanism. Handb Exp Pharmacol, 31–74. 10.1007/978-3-540-79090-7_2.
7. Ford AC, Sperber AD, Corsetti M, and Camilleri M (2020). Irritable bowel syndrome. Lancet 396, 1675–1688. 10.1016/S0140-6736(20)31548-8. [PubMed: 33049223]
8. Rouwette T, Avenali L, Sondermann J, Narayanan P, Gomez-Varela D, and Schmidt M (2015). Modulation of nociceptive ion channels and receptors via protein-protein interactions: implications for pain relief. Channels (Austin) 9, 175–185. 10.1080/19336950.2015.1051270. [PubMed: 26039491]
9. Fuentes IM, and Christianson JA (2016). Ion channels, ion channel receptors, and visceral hypersensitivity in irritable bowel syndrome. Neurogastroenterol Motil 28, 1613–1618. 10.1111/nmo.12979. [PubMed: 27781369]
10. Beyder A, and Farrugia G (2016). Ion channelopathies in functional GI disorders. Am J Physiol Gastrointest Liver Physiol 311, G581–G586. 10.1152/ajpgi.00237.2016. [PubMed: 27514480]
11. Scanzi J, Accarie A, Muller E, Pereira B, Aissouni Y, Goutte M, Joubert-Zakeyh J, Picard E, Boudieu L, Mallet C, et al. (2016). Colonic overexpression of the T-type calcium channel Cav 3.2 in a mouse model of visceral hypersensitivity and in irritable bowel syndrome patients. Neurogastroenterol Motil 28, 1632–1640. 10.1111/nmo.12860. [PubMed: 27196538]
12. Jones RC 3rd, Xu L, and Gebhart GF (2005). The mechanosensitivity of mouse colon afferent fibers and their sensitization by inflammatory mediators require transient receptor potential vanilloid 1 and acid-sensing ion channel 3. J Neurosci 25, 10981–10989. 10.1523/JNEUROSCI.0703-05.2005. [PubMed: 16306411]
13. Schwartz ES, La JH, Scheff NN, Davis BM, Albers KM, and Gebhart GF (2013). TRPV1 and TRPA1 antagonists prevent the transition of acute to chronic inflammation and pain in chronic pancreatitis. J Neurosci 33, 5603–5611. 10.1523/JNEUROSCI.1806-12.2013. [PubMed: 23536075]
14. Ranade SS, Syeda R, and Patapoutian A (2015). Mechanically Activated Ion Channels. Neuron 87, 1162–1179. 10.1016/j.neuron.2015.08.032. [PubMed: 26402601]
15. Nikolaev YA, Cox CD, Ridone P, Rohde PR, Cordero-Morales JF, Vasquez V, Laver DR, and Martinac B (2019). Mammalian TRP ion channels are insensitive to membrane stretch. J Cell Sci 132. 10.1242/jcs.238360.
16. Coste B, Mathur J, Schmidt M, Earley TJ, Ranade S, Petrus MJ, Dubin AE, and Patapoutian A (2010). Piezo1 and Piezo2 are essential components of distinct mechanically activated cation channels. Science 330, 55–60. 10.1126/science.1193270. [PubMed: 20813920]
17. Murthy SE, Loud MC, Daou I, Marshall KL, Schwaller F, Kuhnemund J, Francisco AG, Keenan WT, Dubin AE, Lewin GR, and Patapoutian A (2018). The mechanosensitive ion channel Piezo2 mediates sensitivity to mechanical pain in mice. Sci Transl Med 10. 10.1126/scitranslmed.aat9897.
18. Szczot M, Liljencrantz J, Ghitani N, Barik A, Lam R, Thompson JH, Bharucha-Goebel D, Saade D, Necaise A, Donkervoort S, et al. (2018). PIEZO2 mediates injury-induced tactile pain in mice and humans. Sci Transl Med 10. 10.1126/scitranslmed.aat9892.
19. Hill RZ, Loud MC, Dubin AE, Peet B, and Patapoutian A (2022). PIEZO1 transduces mechanical itch in mice. Nature 607, 104–110. 10.1038/s41586-022-04860-5. [PubMed: 35732741]
20. Cavanaugh DJ, Lee H, Lo L, Shields SD, Zylka MJ, Basbaum AI, and Anderson DJ (2009). Distinct subsets of unmyelinated primary sensory fibers mediate behavioral responses to noxious thermal and mechanical stimuli. Proc Natl Acad Sci U S A 106, 9075–9080. 10.1073/pnas.0901507106. [PubMed: 19451647]
21. Cho WG, and Valtschanoff JG (2008). Vanilloid receptor TRPV1-positive sensory afferents in the mouse ankle and knee joints. Brain Res 1219, 59–65. 10.1016/j.brainres.2008.04.043. [PubMed: 18538749]
22. Avelino A, Cruz C, Nagy I, and Cruz F (2002). Vanilloid receptor 1 expression in the rat urinary tract. Neuroscience 109, 787–798. 10.1016/s0306-4522(01)00496-1. [PubMed: 11927161]
23. Ward SM, Bayguinov J, Won KJ, Grundy D, and Berthoud HR (2003). Distribution of the vanilloid receptor (VR1) in the gastrointestinal tract. J Comp Neurol 465, 121–135. 10.1002/cne.10801. [PubMed: 12926020]

24. Robinson DR, McNaughton PA, Evans ML, and Hicks GA (2004). Characterization of the primary spinal afferent innervation of the mouse colon using retrograde labelling. Neurogastroenterol Motil 16, 113–124. 10.1046/j.1365-2982.2003.00456.x. [PubMed: 14764211]
25. Mishra SK, Tisel SM, Orestes P, Bhangoo SK, and Hoon MA (2011). TRPV1-lineage neurons are required for thermal sensation. EMBO J 30, 582–593. 10.1038/emboj.2010.325. [PubMed: 21139565]
26. Madisen L, Zwingman TA, Sunkin SM, Oh SW, Zariwala HA, Gu H, Ng LL, Palmiter RD, Hawrylycz MJ, Jones AR, et al. (2010). A robust and high-throughput Cre reporting and characterization system for the whole mouse brain. Nat Neurosci 13, 133–140. 10.1038/nn.2467. [PubMed: 20023653]
27. Akbar A, Yiangou Y, Facer P, Walters JR, Anand P, and Ghosh S (2008). Increased capsaicin receptor TRPV1-expressing sensory fibres in irritable bowel syndrome and their correlation with abdominal pain. Gut 57, 923–929. 10.1136/gut.2007.138982. [PubMed: 18252749]
28. Feng J, Yang P, Mack MR, Dryn D, Luo J, Gong X, Liu S, Oetjen LK, Zholos AV, Mei Z, et al. (2017). Sensory TRP channels contribute differentially to skin inflammation and persistent itch. Nat Commun 8, 980. 10.1038/s41467-017-01056-8. [PubMed: 29081531]
29. Lan Z, Chen L, Feng J, Xie Z, Liu Z, Wang F, Liu P, Yue X, Du L, Zhao Y, et al. (2021). Mechanosensitive TRPV4 is required for crystal-induced inflammation. Ann Rheum Dis 80, 1604–1614. 10.1136/annrheumdis-2021-220295. [PubMed: 34663597]
30. Fernandes ES, Fernandes MA, and Keeble JE (2012). The functions of TRPA1 and TRPV1: moving away from sensory nerves. Br J Pharmacol 166, 510–521. 10.1111/j.1476-5381.2012.01851.x. [PubMed: 22233379]
31. Kyloh M, Nicholas S, Zagorodnyuk VP, Brookes SJ, and Spencer NJ (2011). Identification of the visceral pain pathway activated by noxious colorectal distension in mice. Frontiers in neuroscience 5, 16. 10.3389/fnins.2011.00016. [PubMed: 21390285]
32. Ranade SS, Woo SH, Dubin AE, Moshourab RA, Wetzel C, Petrus M, Mathur J, Begay V, Coste B, Mainquist J, et al. (2014). Piezo2 is the major transducer of mechanical forces for touch sensation in mice. Nature 516, 121–125. 10.1038/nature13980. [PubMed: 25471886]
33. Dalghi MG, Ruiz WG, Clayton DR, Montalbetti N, Daugherty SL, Beckel JM, Carattino MD, and Apodaca G (2021). Functional roles for PIEZO1 and PIEZO2 in urothelial mechanotransduction and lower urinary tract interoception. JCI Insight 6. 10.1172/jci.insight.152984.
34. Marshall KL, Saade D, Ghitani N, Coombs AM, Szczot M, Keller J, Ogata T, Daou I, Stowers LT, Bonnemann CG, et al. (2020). PIEZO2 in sensory neurons and urothelial cells coordinates urination. Nature 588, 290–295. 10.1038/s41586-020-2830-7. [PubMed: 33057202]
35. Wang J, La JH, and Hamill OP (2019). PIEZO1 Is Selectively Expressed in Small Diameter Mouse DRG Neurons Distinct From Neurons Strongly Expressing TRPV1. Front Mol Neurosci 12, 178. 10.3389/fnmol.2019.00178. [PubMed: 31379500]
36. Roh J, Hwang SM, Lee SH, Lee K, Kim YH, and Park CK (2020). Functional Expression of Piezo1 in Dorsal Root Ganglion (DRG) Neurons. International journal of molecular sciences 21. 10.3390/ijms21113834.
37. Coutinho SV, and Gebhart GF (1999). A role for spinal nitric oxide in mediating visceral hyperalgesia in the rat. Gastroenterology 116, 1399–1408. 10.1016/s0016-5085(99)70504-4. [PubMed: 10348823]
38. Feng B, La JH, Schwartz ES, Tanaka T, McMurray TP, and Gebhart GF (2012). Long-term sensitization of mechanosensitive and -insensitive afferents in mice with persistent colorectal hypersensitivity. American journal of physiology. Gastrointestinal and liver physiology 302, G676–683. 10.1152/ajpgi.00490.2011. [PubMed: 22268098]
39. Jones RC 3rd, Otsuka E, Wagstrom E, Jensen CS, Price MP, and Gebhart GF (2007). Short-term sensitization of colon mechanoreceptors is associated with long-term hypersensitivity to colon distention in the mouse. Gastroenterology 133, 184–194. 10.1053/j.gastro.2007.04.042. [PubMed: 17553498]
40. Cappell MS, and Batke M (2008). Mechanical obstruction of the small bowel and colon. Med Clin North Am 92, 575–597, viii. 10.1016/j.mcna.2008.01.003. [PubMed: 18387377]

41. Huang TY, and Hanani M (2005). Morphological and electrophysiological changes in mouse dorsal root ganglia after partial colonic obstruction. Am J Physiol Gastrointest Liver Physiol 289, G670–678. 10.1152/ajpgi.00028.2005. [PubMed: 15920014]
42. Cho H, Jang Y, Lee B, Chun H, Jung J, Kim SM, Hwang SW, and Oh U (2013). Voluntary movements as a possible non-reflexive pain assay. Mol Pain 9, 25. 10.1186/1744-8069-9-25. [PubMed: 23688027]
43. Spencer NJ, Magnusdottir EI, Jakobsson J, Kestell G, Nan Chen B, Morris D, Brookes SJH, and Lagerstrom MC (2017). CGRPalpha within the Trpv1-Cre population contributes to visceral nociception. Am J Physiol Gastrointest Liver Physiol, ajpgi 00188 02017. 10.1152/ajpgi.00188.2017.
44. Xie Z, Feng J, Cai T, McCarthy R, Eschbach MD 2nd, Wang Y, Zhao Y, Yi Z, Zang K, Yuan Y, et al. (2022). Estrogen metabolites increase nociceptor hyperactivity in a mouse model of uterine pain. JCI insight 7. 10.1172/jci.insight.149107.
45. de la Puente B, Zamanillo D, Romero L, Vela JM, Merlos M, and Portillo-Salido E (2017). Pharmacological sensitivity of reflexive and nonreflexive outcomes as a correlate of the sensory and affective responses to visceral pain in mice. Sci Rep 7, 13428. 10.1038/s41598-017-13987-9. [PubMed: 29044171]
46. Cseko K, Beckers B, Keszthelyi D, and Helyes Z (2019). Role of TRPV1 and TRPA1 Ion Channels in Inflammatory Bowel Diseases: Potential Therapeutic Targets? Pharmaceuticals (Basel) 12. 10.3390/ph12020048.
47. Perna E, Aguilera-Lizarraga J, Florens MV, Jain P, Theofanous SA, Hanning N, De Man JG, Berg M, De Winter B, Alpizar YA, et al. (2021). Effect of resolvins on sensitisation of TRPV1 and visceral hypersensitivity in IBS. Gut 70, 1275–1286. 10.1136/gutjnl-2020-321530. [PubMed: 33023902]
48. Defaye M, Abdullah NS, Iftinca M, Hassan A, Agosti F, Zhang Z, Cumenal M, Zamponi GW, and Altier C (2021). Gut-innervating TRPV1+ neurons drive chronic visceral pain via microglial P2Y12 receptor. Cell Mol Gastroenterol Hepatol. 10.1016/j.jcmgh.2021.12.012.
49. Makadia PA, Najjar SA, Saloman JL, Adelman P, Feng B, Margiotta JF, Albers KM, and Davis BM (2018). Optogenetic Activation of Colon Epithelium of the Mouse Produces High-Frequency Bursting in Extrinsic Colon Afferents and Engages Visceromotor Responses. J Neurosci 38, 5788–5798. 10.1523/JNEUROSCI.0837-18.2018. [PubMed: 29789376]
50. Story GM, Peier AM, Reeve AJ, Eid SR, Mosbacher J, Hricik TR, Earley TJ, Hergarden AC, Andersson DA, Hwang SW, et al. (2003). ANKTM1, a TRP-like channel expressed in nociceptive neurons, is activated by cold temperatures. Cell 112, 819–829. 10.1016/s0092-8674(03)00158-2. [PubMed: 12654248]
51. Bautista DM, Jordt SE, Nikai T, Tsuruda PR, Read AJ, Poblete J, Yamoah EN, Basbaum AI, and Julius D (2006). TRPA1 mediates the inflammatory actions of environmental irritants and proalgesic agents. Cell 124, 1269–1282. 10.1016/j.cell.2006.02.023. [PubMed: 16564016]
52. Hockley JRF, Taylor TS, Callejo G, Wilbrey AL, Gutteridge A, Bach K, Winchester WJ, Bulmer DC, McMurray G, and Smith ESJ (2019). Single-cell RNAseq reveals seven classes of colonic sensory neuron. Gut 68, 633–644. 10.1136/gutjnl-2017-315631. [PubMed: 29483303]
53. Meerschaert KA, Adelman PC, Friedman RL, Albers KM, Koerber HR, and Davis BM (2020). Unique Molecular Characteristics of Visceral Afferents Arising from Different Levels of the Neuraxis: Location of Afferent Somata Predicts Function and Stimulus Detection Modalities. The Journal of neuroscience : the official journal of the Society for Neuroscience 40, 7216–7228. 10.1523/JNEUROSCI.1426-20.2020. [PubMed: 32817244]
54. Borbiro I, Badheka D, and Rohacs T (2015). Activation of TRPV1 channels inhibits mechanosensitive Piezo channel activity by depleting membrane phosphoinositides. Sci Signal 8, ra15. 10.1126/scisignal.2005667. [PubMed: 25670203]
55. Weng HJ, Patel KN, Jeske NA, Bierbower SM, Zou W, Tiwari V, Zheng Q, Tang Z, Mo GC, Wang Y, et al. (2015). Tmem100 Is a Regulator of TRPA1-TRPV1 Complex and Contributes to Persistent Pain. Neuron 85, 833–846. 10.1016/j.neuron.2014.12.065. [PubMed: 25640077]
56. Akopian AN (2011). Regulation of nociceptive transmission at the periphery via TRPA1-TRPV1 interactions. Curr Pharm Biotechnol 12, 89–94. 10.2174/138920111793937952. [PubMed: 20932255]

57. Masuoka T, Kudo M, Yamashita Y, Yoshida J, Imaizumi N, Muramatsu I, Nishio M, and Ishibashi T (2017). TRPA1 Channels Modify TRPV1-Mediated Current Responses in Dorsal Root Ganglion Neurons. Front Physiol 8, 272. 10.3389/fphys.2017.00272. [PubMed: 28515697]
58. Matsunami M, Kirishi S, Okui T, and Kawabata A (2011). Chelating luminal zinc mimics hydrogen sulfide-evoked colonic pain in mice: possible involvement of T-type calcium channels. Neuroscience 181, 257–264. 10.1016/j.neuroscience.2011.02.044. [PubMed: 21354272]
59. Matsunami M, Miki T, Nishiura K, Hayashi Y, Okawa Y, Nishikawa H, Sekiguchi F, Kubo L, Ozaki T, Tsujiuchi T, and Kawabata A (2012). Involvement of the endogenous hydrogen sulfide/Ca(v) 3.2 T-type Ca2+ channel pathway in cystitis-related bladder pain in mice. British journal of pharmacology 167, 917–928. 10.1111/j.1476-5381.2012.02060.x. [PubMed: 22646666]
60. Marger F, Gelot A, Alloui A, Matricon J, Ferrer JF, Barrere C, Pizzoccaro A, Muller E, Nargeot J, Snutch TP, et al. (2011). T-type calcium channels contribute to colonic hypersensitivity in a rat model of irritable bowel syndrome. Proceedings of the National Academy of Sciences of the United States of America 108, 11268–11273. 10.1073/pnas.1100869108. [PubMed: 21690417]
61. Picard E, Carvalho FA, Agosti F, Bourinet E, Ardid D, Eschalier A, Daulhac L, and Mallet C (2019). Inhibition of Cav 3.2 calcium channels: A new target for colonic hypersensitivity associated with low-grade inflammation. British journal of pharmacology 176, 950–963. 10.1111/bph.14608. [PubMed: 30714145]
62. Chesler AT, Szczot M, Bharucha-Goebel D, Ceko M, Donkervoort S, Laubacher C, Hayes LH, Alter K, Zampieri C, Stanley C, et al. (2016). The Role of PIEZO2 in Human Mechanosensation. N Engl J Med 375, 1355–1364. 10.1056/NEJMoa1602812. [PubMed: 27653382]
63. Case LK, Liljencrantz J, Madian N, Necaise A, Tubbs J, McCall M, Bradson ML, Szczot M, Pitcher MH, Ghitani N, et al. (2021). Innocuous pressure sensation requires A-type afferents but not functional RhoIotaEpsilonZetaOmicron2 channels in humans. Nat Commun 12, 657. 10.1038/s41467-021-20939-5. [PubMed: 33510158]
64. Nagi SS, Marshall AG, Makdani A, Jarocka E, Liljencrantz J, Ridderstrom M, Shaikh S, O'Neill F, Saade D, Donkervoort S, et al. (2019). An ultrafast system for signaling mechanical pain in human skin. Sci Adv 5, eaaw1297. 10.1126/sciadv.aaw1297. [PubMed: 31281886]
65. Aguilera-Lizarraga J, Florens MV, Viola MF, Jain P, Decraecker L, Appeltans I, Cuende-Estevez M, Fabre N, Van Beek K, Perna E, et al. (2021). Local immune response to food antigens drives meal-induced abdominal pain. Nature 590, 151–156. 10.1038/s41586-020-03118-2. [PubMed: 33442055]
66. Dodds KN, Beckett EA, Evans SF, Grace PM, Watkins LR, and Hutchinson MR (2016). Glial contributions to visceral pain: implications for disease etiology and the female predominance of persistent pain. Translational psychiatry 6, e888. 10.1038/tp.2016.168. [PubMed: 27622932]
67. Dubin AE, Schmidt M, Mathur J, Petrus MJ, Xiao B, Coste B, and Patapoutian A (2012). Inflammatory signals enhance piezo2-mediated mechanosensitive currents. Cell reports 2, 511–517. 10.1016/j.celrep.2012.07.014. [PubMed: 22921401]
68. Luo Z, Liao X, Luo L, Fan Q, Zhang X, Guo Y, Wang F, Ye Z, and Luo D (2021). Extracellular ATP and cAMP signaling promote Piezo2-dependent mechanical allodynia after trigeminal nerve compression injury. J Neurochem. 10.1111/jnc.15537.
69. Nencini S, Morgan M, Thai J, Jobling AI, Mazzone SB, and Ivanusic JJ (2021). Piezo2 Knockdown Inhibits Noxious Mechanical Stimulation and NGF-Induced Sensitization in A-Delta Bone Afferent Neurons. Front Physiol 12, 644929. 10.3389/fphys.2021.644929. [PubMed: 34335288]
70. Prato V, Taberner FJ, Hockley JRF, Callejo G, Arcourt A, Tazir B, Hammer L, Schad P, Heppenstall PA, Smith ES, and Lechner SG (2017). Functional and Molecular Characterization of Mechanoinsensitive "Silent" Nociceptors. Cell reports 21, 3102–3115. 10.1016/j.celrep.2017.11.066. [PubMed: 29241539]
71. Eijkelkamp N, Linley JE, Torres JM, Bee L, Dickenson AH, Gringhuis M, Minett MS, Hong GS, Lee E, Oh U, et al. (2013). A role for Piezo2 in EPAC1-dependent mechanical allodynia. Nat Commun 4, 1682. 10.1038/ncomms2673. [PubMed: 23575686]
72. Del Rosario JS, Yudin Y, Su S, Hartle CM, Mirshahi T, and Rohacs T (2020). Gi-coupled receptor activation potentiates Piezo2 currents via Gbetagamma. EMBO Rep 21, e49124. 10.15252/embr.201949124. [PubMed: 32227462]

73. Feng B, and Gebhart GF (2015). In vitro functional characterization of mouse colorectal afferent endings. Journal of visualized experiments : JoVE, 52310. 10.3791/52310.

Highlights

1. Piezo2 channels in TRPV1^{+} visceral afferents contribute to colonic mechanosensation.
2. Piezo2 channels contribute to mechanically-induced visceral pain signaling in mice.
3. Ablation or inhibition of Piezo2 function ameliorates visceral hypersensitivity.
4. Piezo2 could be a therapeutic target to silencing the gut-brain axis.

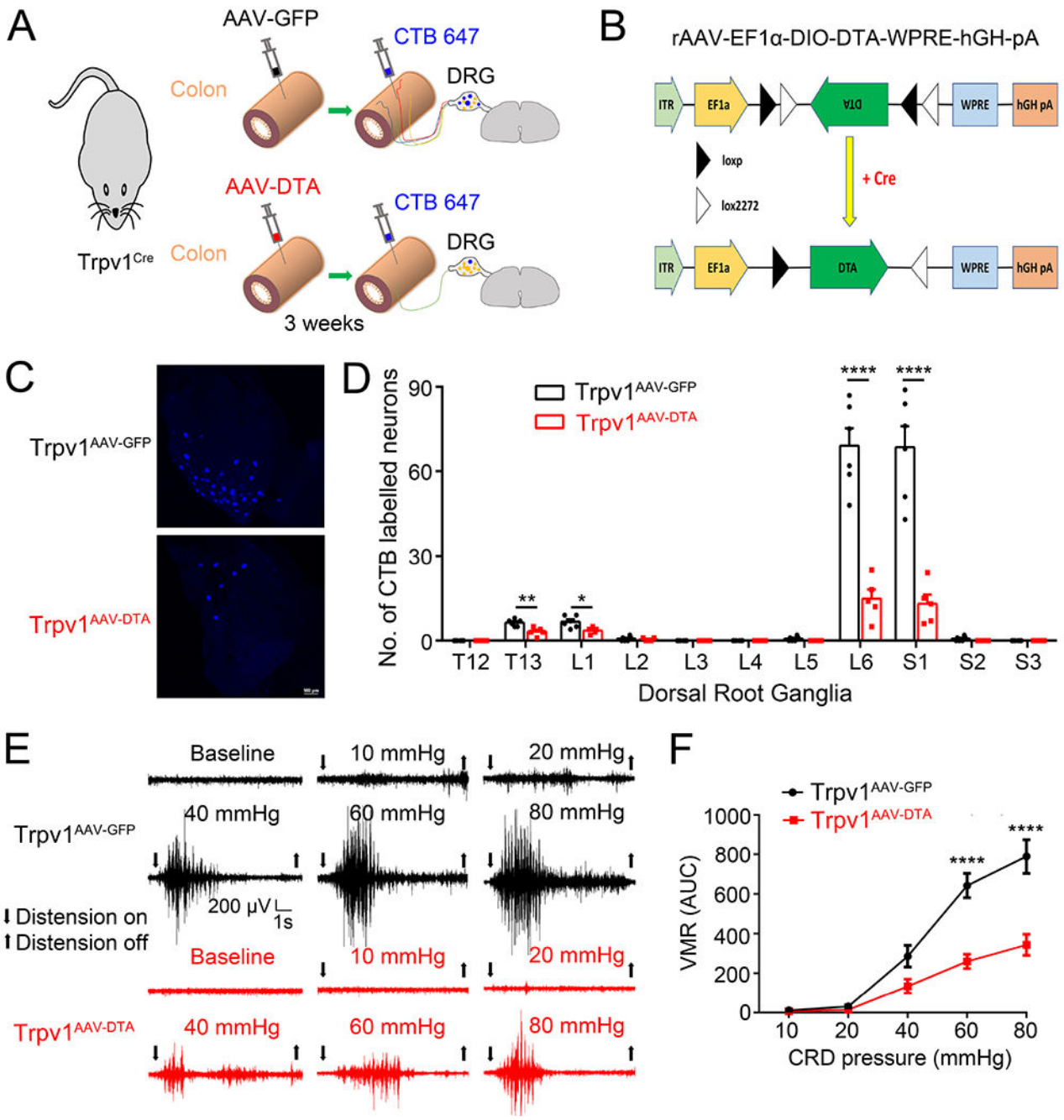

Figure 1. Virally-mediated ablation of colon-innervating TRPV1-expressing nociceptors attenuates CRD-induced VMR.

(**A**). Schematic representation of intracolonic injections of AAV encoding GFP or DTA into the Trpv1^{Cre} mice followed by intracolonic injections of CTB 647 for retrograde labeling. (**B**). Schematic diagram illustrating the AAV-EF1α-DIO-DTA construct that expresses diphtheria toxin subunit A (DTA) in a Cre-dependent configuration to cause selective cell death in Cre-expressing neurons. (**C, D**). Representative images **(C)** and quantification **(D)** of retrogradely-labeled DRG neurons following injection of CTB-647 into the distal colon of

TRPV1$^{AAV\text{-}GFP}$ and TRPV1$^{AAV\text{-}DTA}$ mice *P < 0.05, **p < 0.01, ****P < 0.0001, Statistical analyses by two-way ANOVA, with post hoc independent-samples t-test with FDR (False Discovery Rate) correction to compare T13, L1, L2, L5, L6, S1 and S2. (**E**). Representative electromyogram recordings elicited by graded CRD pressures (10, 20, 40, 60 and 80 mmHg) recorded from TRPV1$^{AAV\text{-}GFP}$ mice and TRPV1$^{AAV\text{-}DTA}$ mice. (**F**). Summary data showing that TRPV1$^{AAV\text{-}DTA}$ mice display significantly decreased VMR to CRD compared with TRPV1$^{AAV\text{-}GFP}$ mice at distension pressures of 60 mmHg and 80 mmHg. ****P < 0.0001, two-way ANOVA, n=5 mice per group. All data are expressed as means ± S.E.

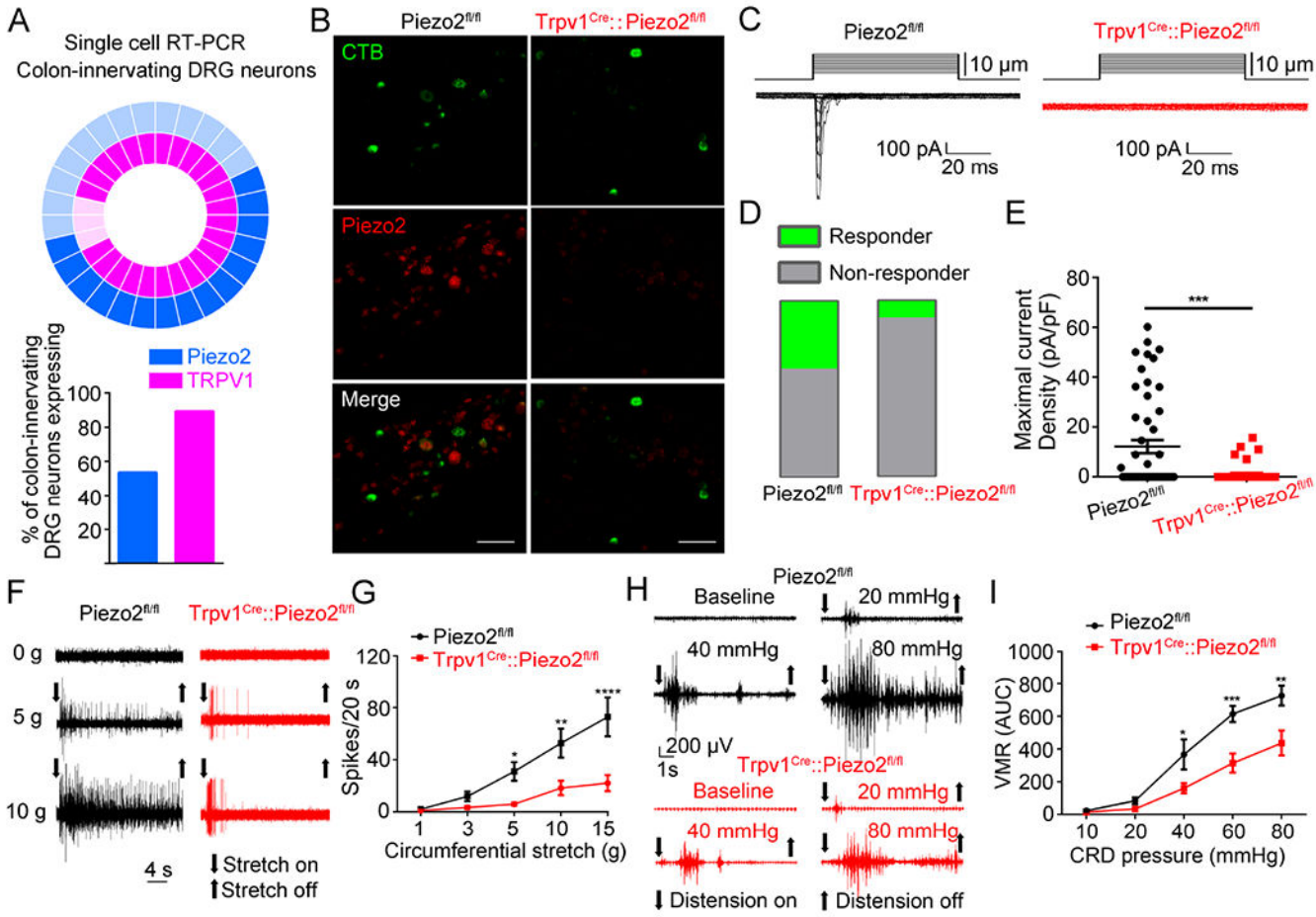

Figure 2. Conditional knockout of Piezo2 from TRPV1-lineage neurons attenuates visceral mechanosensitivity and nociception.

(**A**). Donut plot showing expression and co-expression of *Piezo2* and *Trpv1* in 28 individual retrogradely traced colon-innervating LS DRG neurons. Each color represents an individual gene with expression marked by bold shading (upper panel). *Piezo2* is represented in the outer ring, with *Trpv1* in the inner ring. Summary data of single-cell qRT-PCR of retrogradely labeled colon-innervating DRG neurons reveal the percentage of neurons expressing *Piezo2* and *Trpv1* (lower panel; n=28 cells from 5 mice). (**B**). Representative images of *Piezo2* in situ hybridization in L6 DRG sections from Piezo2$^{fl/fl}$ (left) and Trpv1^{Cre}::Piezo2$^{fl/fl}$ (right) mice. Green, CTB488; Red, *Piezo2* transcript. Images shown here were representative of three independent experiments using tissues from three different mice. Scale bar=100 μm. (**C**). Representative whole-cell MA current traces elicited by mechanical indentation in retrogradely labeled CTB 488^{+} colon-innervating DRG neurons isolated from Piezo2$^{fl/fl}$ and Trpv1^{Cre}::Piezo2$^{fl/fl}$ mice. (**D-E).** The proportions of DRG neurons (**D**) responding with whole-cell MA currents and maximal current density (**E**) of inward whole-cell MA currents elicited at a holding potential of −80 mV in colon-innervating DRG neurons isolated from Piezo2$^{fl/fl}$ and Trpv1^{Cre}::Piezo2$^{fl/fl}$ mice. Data are expressed as mean ± S.E. ***P<0.001, unpaired *t* test. n=52 cells from 8 mice for Piezo2$^{fl/fl}$ group; n=51 cells from 7 mice for Trpv1^{Cre}::Piezo2$^{fl/fl}$ group. (**F**). Representative

traces of colon pelvic nerve recordings from Piezo2$^{fl/fl}$ and Trpv1^{Cre}::Piezo2$^{fl/fl}$ mice. (**G**). Summary data of colon pelvic nerve recording of Piezo2$^{fl/fl}$ and Trpv1^{Cre}::Piezo2$^{fl/fl}$ mice in response to graded circumferential stretch (1, 3, 5, 10, and 15g). *P < 0.05, **P <0.01, ****P < 0.0001, two-way ANOVA, n=15 units from 5 mice for Piezo2$^{fl/fl}$ group and n=17 units from 6 mice for Trpv1^{Cre}::Piezo2$^{fl/fl}$ group. (**H**). Representative electromyogram recordings induced by graded CRD pressures (10, 20, 40, 60 and 80 mmHg) in Piezo2$^{fl/fl}$ and Trpv1^{Cre}::Piezo2$^{fl/fl}$ mice. (**I**). Trpv1^{Cre}::Piezo2$^{fl/fl}$ mice displayed significantly reduced CRD-induced VMRs compared to Piezo2$^{fl/fl}$ mice. *P<0.05, **P<0.01, ***P<0.001, two-way ANOVA, n=6 to 7 mice per group. All data are expressed as mean ± S.E.

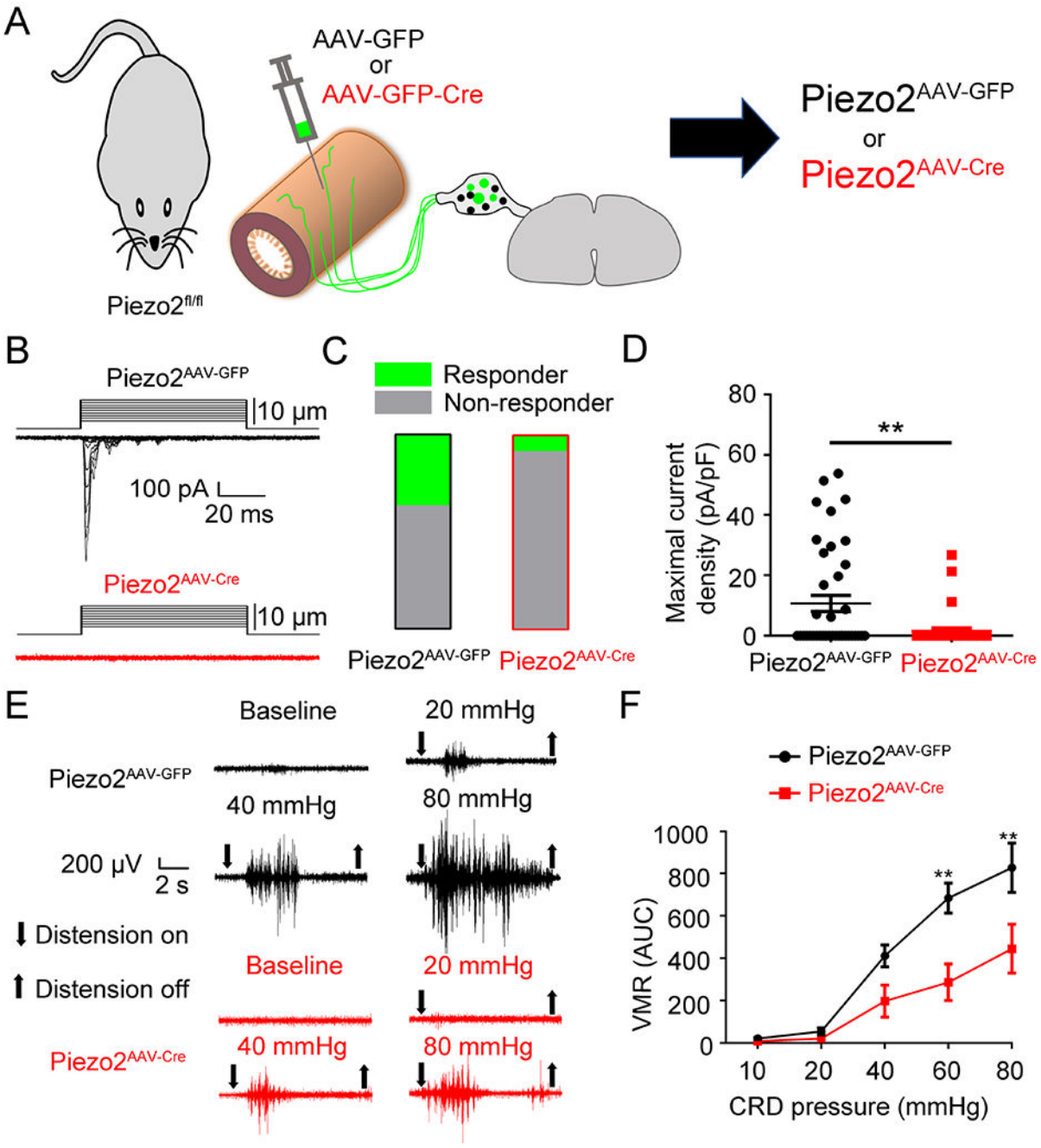

Figure 3. Virally-mediated knockdown of Piezo2 function from colon-innervating DRG neurons reduces visceral mechanosensitivity and nociception.

(**A**). Schematic representation of intracolonic injection of AAV encoding GFP or GFP-Cre into Piezo2$^{fl/fl}$ mice. (**B**). Representative whole-cell MA currents in response to mechanical indentation in GFP^{+} DRG neurons isolated from Piezo2$^{AAV\text{-}GFP}$ and Piezo2$^{AAV\text{-}GFP\text{-}Cre}$mice. (**C**). Proportions of DRG neurons responding with whole-cell MA currents in Piezo2$^{AAV\text{-}GFP}$ and Piezo2$^{AAV\text{-}GFP\text{-}Cre}$ mice. n=41 cells from 5 mice for Piezo2$^{AAV\text{-}GFP}$ and n=37 cells from 5 mice for Piezo2$^{AAV\text{-}GFP\text{-}Cre}$. **(D)**. Maximal

current density of inward whole-cell MA currents elicited at a holding potential of −80 mV in DRG neurons from Piezo2$^{AAV\text{-}GFP}$ and Piezo2$^{AAV\text{-}GFP\text{-}Cre}$ mice. **P < 0.01, two-tailed Student's *t*-test. n=41 cells from 5 mice for Piezo2$^{AAV\text{-}GFP}$ and n=37 cells from 5 mice for Piezo2$^{AAV\text{-}GFP\text{-}Cre}$. (**E**). Representative electromyogram recording elicited by graded CRD pressures in Piezo2$^{AAV\text{-}GFP}$ mice and Piezo2$^{AAV\text{-}GFP\text{-}Cre}$ mice. **(F)**. Summary data showing that Piezo2$^{AAV\text{-}GFP\text{-}Cre}$ mice displayed significantly decreased CRD-induced VMRs compared with Piezo2$^{AAV\text{-}GFP}$ mice at distension pressures of 60 mmHg and 80 mmHg. **P < 0.01, two-way ANOVA, n=5 mice per group. All data are expressed as means ± S.E.

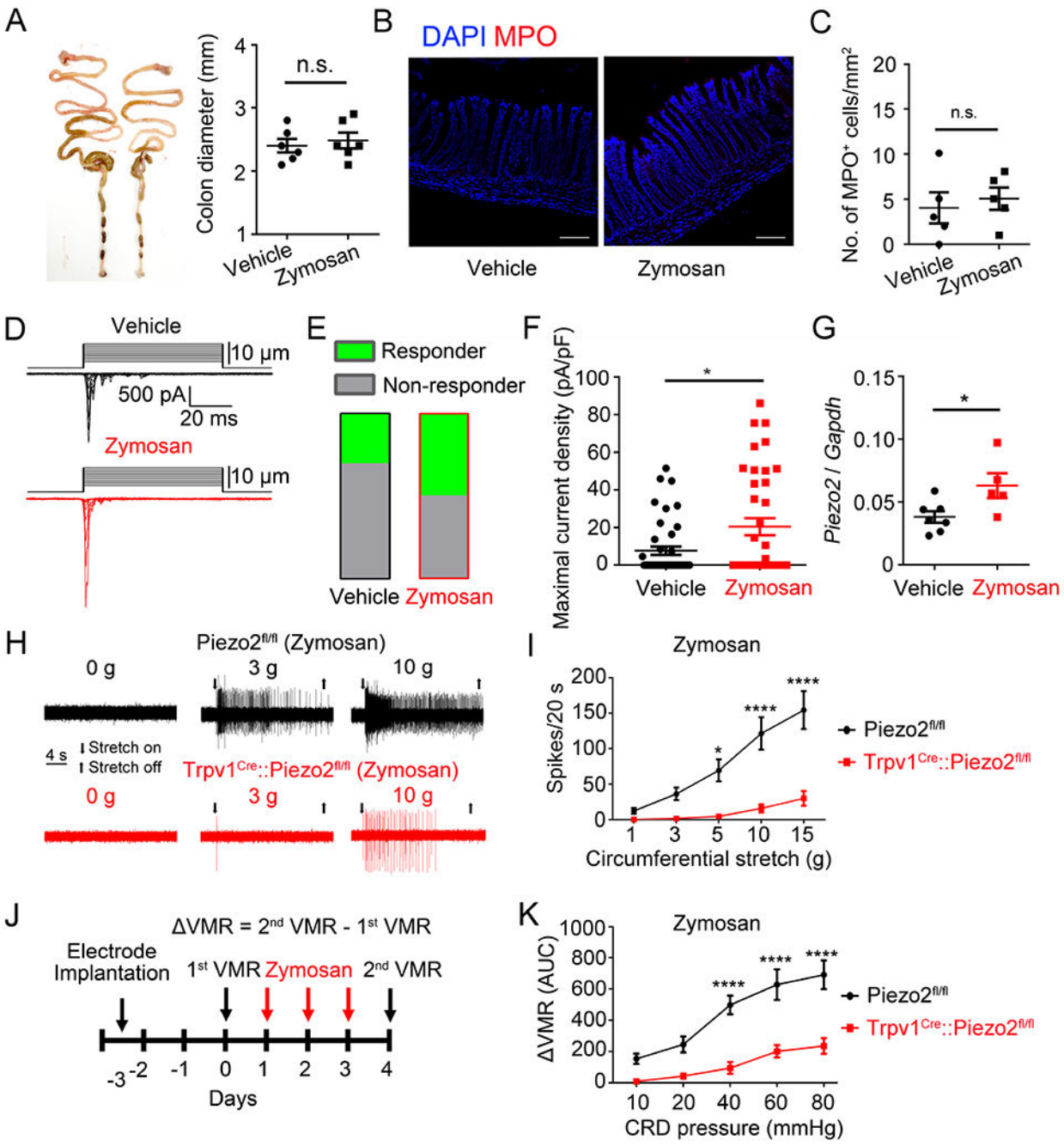

Figure 4. Piezo2 contributes to visceral hypersensitivity in a mouse model zymosan-induced IBS.

(**A**). Representative images of colon preparations from vehicle- and zymosan-treated mice. Note the zymosan-treatment did not cause overt structural changes compared to vehicle-treated mice, n.s., no significant difference, unpaired *t* test, n=6. (**B**). Double labeling of DAPI (blue) and MPO (red) in colon preparations from vehicle- (left) and zymosan-treated (right) mice. Images shown here were representative of three independent experiments. Scale bar=100 μm. (**C**). Statistical data showing comparable numbers of MPO^+ cells in zymosan-treated mice compared to the Sham-treated mice, n.s., no significant difference,

unpaired *t* test, n=5 tissues from 5 mice. **(D)**. Representative traces of whole-cell MA currents elicited by membrane displacement steps from CTB 488^{+} colon-innervating DRG neurons isolated from vehicle-treated and zymosan-treated mice. (**E**). Summary data of the proportions of DRG neurons responding with whole-cell MA currents in vehicle-treated and zymosan-treated mice. n=43 cells from 5 mice for vehicle group and n=38 cells from 5 mice for zymosan group. (**F**). Summary data of the maximal current density of inward whole-cell MA currents elicited at a holding potential of −80 mV in response to mechanical indentation. *P<0.05, unpaired *t* test. n=43 cells from 5 mice for vehicle-treated group and n=38 cells from 5 mice for zymosan-treated group. (**G**) Quantitative RT-PCR analysis of Piezo2 in L6 and S1 DRGs after zymosan treatment. *P<0.05, unpaired *t* test. n=7 mice for vehicle group and n=5 mice for zymosan group. **(H)**. Representative traces of colon pelvic nerve recording of $Piezo2^{fl/fl}$ and $Trpv1^{Cre}$::$Piezo2^{fl/fl}$ mice subjected to zymosan treatment. (**I**). Summary data of stretch stimuli-induced nerve firings of colon nerve recording in $Piezo2^{fl/fl}$ and $Trpv1^{Cre}$::$Piezo2^{fl/fl}$ mice subjected to zymosan treatment. *P<0.05; ****P<0.0001, two-way ANOVA. n=14 units from 4 mice for $Piezo2^{fl/fl}$ group and n=7 units from 3 mice for $Trpv1^{Cre}$::$Piezo2^{fl/fl}$ group. **(J)**. Schematic diagram showing the timing of zymosan treatment and VMR recording. **(K)**. Summary data showing that zymosan-induced visceral hypersensitivity is significantly reduced in $Trpv1^{Cre}$::$Piezo2^{fl/fl}$ mice compared to that in $Piezo2^{fl/fl}$ mice. ****P<0.0001, two-way ANOVA, n=5 mice per group. All data are expressed as mean ± S.E.

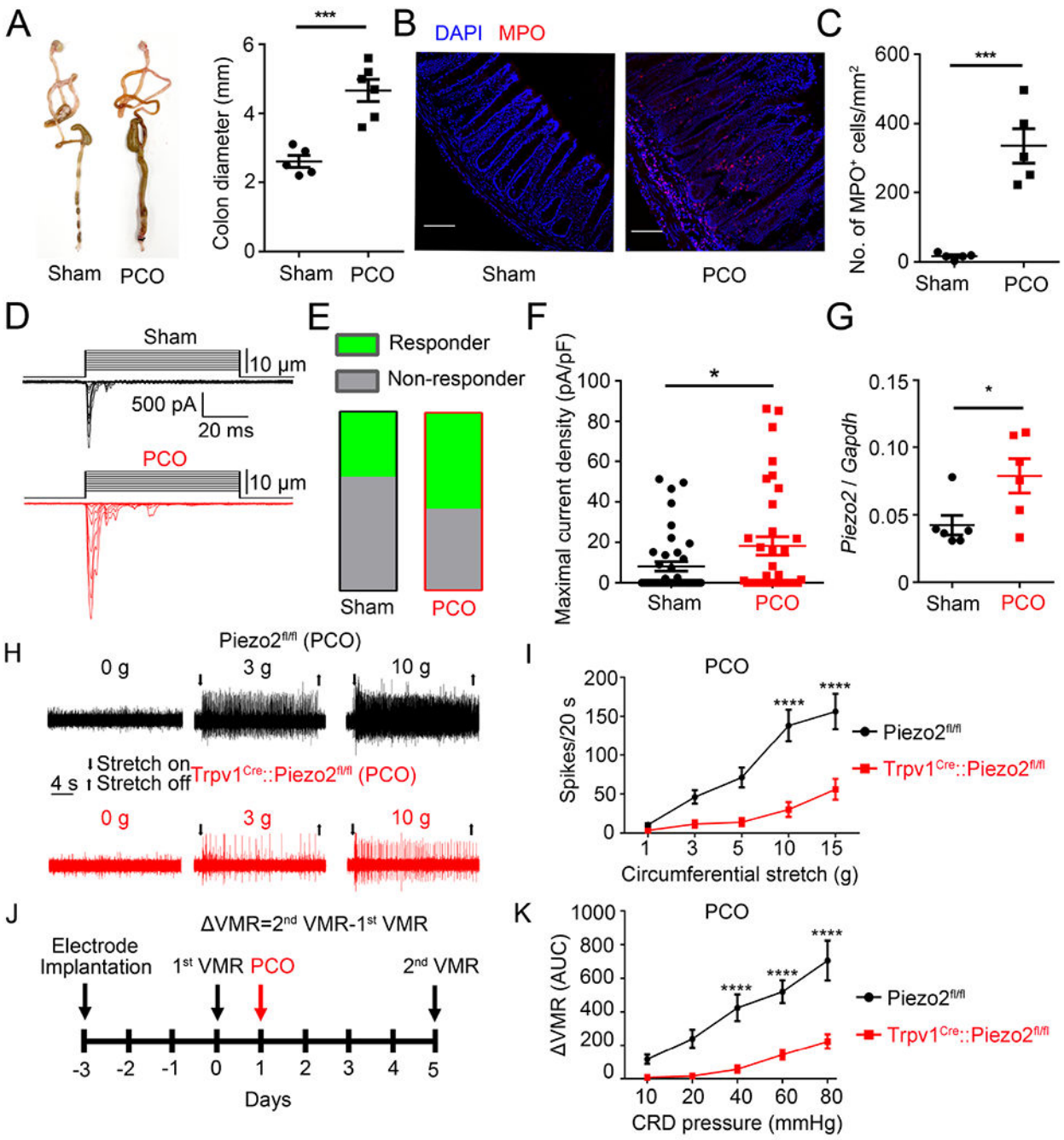

Figure 5. Piezo2 mediates visceral mechanical hypersensitivity in a mouse model of PCO.

(**A**). Representative images of colon preparations from sham- and PCO-treated mice. Note the PCO-treated mice showed increased colonic diameter compared to sham-treated mice. ***P < 0.001, unpaired *t* test, n=5-6 per group. (**B**). Double labeling of DAPI (blue) and MPO (red) in colon preparations from sham- (left) and PCO-treated (right) mice. Images shown here were representative of three independent experiments. Scale bar=100 μm. **(C)**. Statistical data illustrating a statistically significant increase of MPO^+ cells in PCO-treated mice compared to the sham-treated mice. ***P < 0.001, unpaired *t* test, n=5 per group.

(D). Representative traces of whole-cell MA currents elicited by membrane displacement steps from CTB 488^{+} colon-innervating DRG neurons isolated from sham- and PCO-treated mice. (**E**). Proportions of DRG neurons that had MA currents in sham- and PCO-treated mice. n=41 cells from 5 mice for sham-treated group and n=35 cells from 5 mice for PCO-treated group. **(F)**. Summary data of the maximal current density of inward whole-cell MA currents recorded at a holding potential of −80 mV in response to mechanical indentation in Sham- and PCO-treated mice. *P<0.05, unpaired *t* test, n=41 cells from 5 mice for sham group and n=35 cells from 5 mice for PCO group. **(G)** Quantitative RT-PCR analysis of Piezo2 expression in L6 and S1 DRGs after PCO procedure. *P<0.05, unpaired *t* test. n=6 mice for each group. **(H)**. Representative traces of colon pelvic nerve recordings from $Piezo2^{fl/fl}$ and $Trpv1^{Cre}$::$Piezo2^{fl/fl}$ PCO-treated mice. (**I**). Summary data of colonic stretch-evoked pelvic nerve firing in $Piezo2^{fl/fl}$ and $Trpv1^{Cre}$::$Piezo2^{fl/fl}$ PCO-treated mice. ****P<0 0001, Two-way ANOVA, n=27 units from 7 mice for $Piezo2^{fl/fl}$ group and n=13 units from 5 mice for $Trpv1^{Cre}$::$Piezo2^{fl/fl}$ group. **(J)**. Schematic diagram showing the timing of PCO procedure and VMR recording. **(K)**. Summary data showing that PCO-induced visceral hypersensitivity is significantly reduced in $Trpv1^{Cre}$::$Piezo2^{fl/fl}$ mice compared to in $Piezo2^{fl/fl}$mice. ****P<0.0001. Two-way ANOVA, n=6 mice per group. All data are expressed as mean ± S.E.

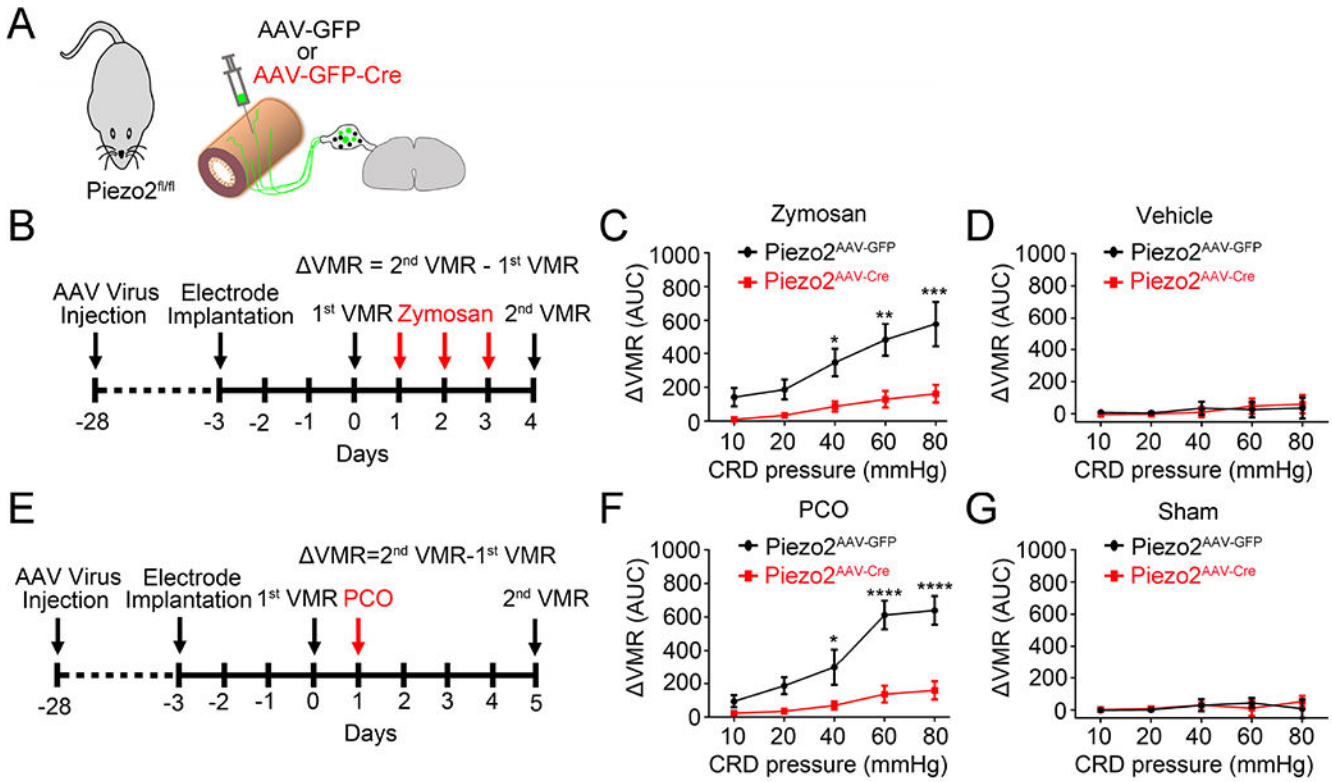

Figure 6. Virally-mediated knockdown of Piezo2 function from colon-innervating DRG neurons reduces visceral hypersensitivity induced by zymosan and PCO.

(**A**). Schematic representation of intracolonic injection of AAV encoding GFP or GFP-Cre into Piezo2$^{fl/fl}$ mice. (**B**). Schematic diagram showing the timing of AAV injection, zymosan treatment, and VMR recording. (**C**) Summary data showing that Piezo2$^{AAV\text{-}DTA}$ mice display significantly decreased zymosan-induced visceral hypersensitivity compared to Piezo2$^{AAV\text{-}GFP}$ mice. *P<0.05, **P<0.01, ***P<0.001. Two-way ANOVA, n=5 mice per group. (**D**) Summary data showing that neither Piezo2$^{AAV\text{-}GFP}$ nor Piezo2$^{AAV\text{-}DTA}$ mice display visceral hypersensitivity after vehicle treatment. n=4 mice per group (**E**). Schematic diagram showing the timing of AAV injection, PCO surgery, and VMR recording. (**F**) Summary data showing that Piezo2$^{AAV\text{-}DTA}$ mice display significantly decreased visceral hypersensitivity induced by PCO compared to Piezo2$^{AAV\text{-}GFP}$ mice. *P<0.05, ****P<0.0001. Two-way ANOVA, n=5 mice per group. (**G**) Summary data showing that neither Piezo2$^{AAV\text{-}GFP}$ nor Piezo2$^{AAV\text{-}DTA}$ mice display visceral hypersensitivity after sham surgery. n=4 mice per group. All data are expressed as mean ± S.E.

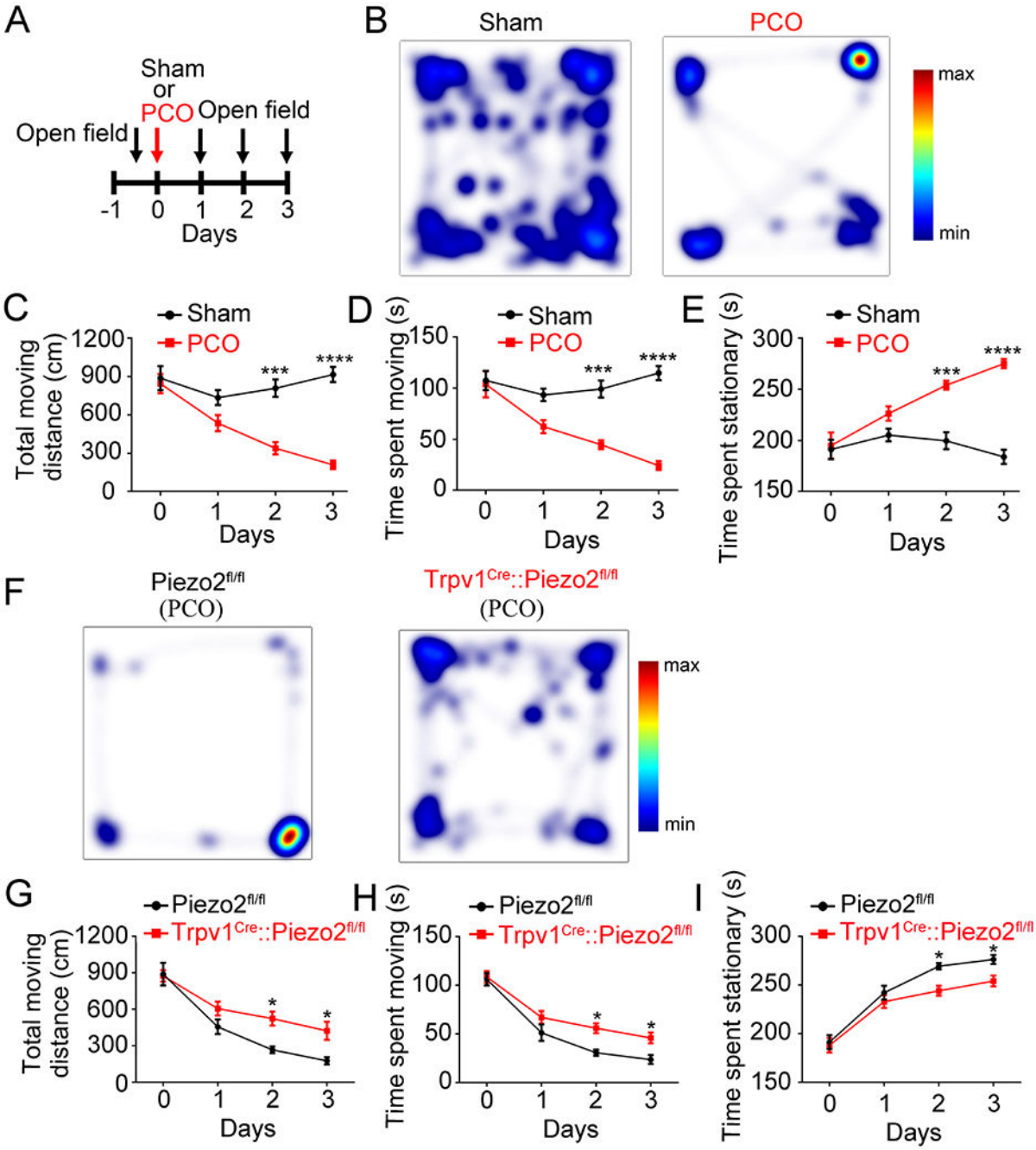

Figure 7. PCO causes a pain-related reduction in voluntary movement which is partially prevented by genetic ablation of Piezo2 function.

(**A**). Schematic representation of PCO procedure and open field recording. (**B**). Representative images illustrating heat maps of voluntary movements of sham- and PCO-treated wild type C57BL/6J mice. (**C-E**). PCO procedure markedly reduced total moving distance (**C**), and total time spent moving (**D**), but increased total time spent stationary (**E**). ***P<0.001, ****P<0.0001, two-way ANOVA, n=6 mice per group. (**F**). Representative images illustrating heat maps of voluntary movements in Piezo2$^{fl/fl}$

(left) and Trpv1^{Cre}::Piezo2$^{fl/fl}$ (right) mice after PCO surgery in open field test. (**G-I**). Trpv1^{Cre}::Piezo2$^{fl/fl}$ mice showed increased total moving distance (**G**) and time spent moving (**H**) and decreased time spent stationary (**I**) compared with Piezo2$^{fl/fl}$ mice. *P<0.05, two-way ANOVA, n=6 mice per group. All data are expressed as mean ± S.E.

Key resources table

REAGENT or RESOURCE	SOURCE	IDENTIFIER
Antibodies		
MPO	Dako Omnis	Cat#: A0398
Virus strains and CTB		
pENN.AAV.hSyn.HI.eGFP-Cre.WPRE.SV40	James M. Wilson lab	Addgene Cat#: 105540
pAAV-hSyn-EGFP	Bryan Roth lab	Addgene Cat#: 50465
rAAV-EF1α-DIO-DTA-WPRE-hGH-pA	BrainVTA	Cat#: PT-0345
rAAV-EF1α-DIO-EGFP-WPRE-hGH-pA	BrainVTA	Cat#: PT-0795
CTB488	Invitrogen	Cat#: C34775
CTB647	Invitrogen	Cat#: C34778
Chemicals, peptides, and recombinant proteins		
Zymosan	Sigma Aldrich	Cat#: Z4250
Ibuprofen	Sigma Aldrich	Cat#: I4883
GsMTx4	Tocris Bioscience	Cat#: 4912
Critical commercial assays		
Single Cell-to-CT™ qRT-PCR Kit	Invitrogen	Cat#: 4458237
Experimental models: Organisms/strains		
C57BL/6J	The Jackson Laboratory	RRID:IMSR_JAX:000664
$Trpv1^{Cre}$	Mark A Hoon lab	N/A
B6.Cg-*Gt(ROSA)26Sor*$^{tm9(CAG\text{-}tdTomato)Hze}$/J	The Jackson Laboratory	RRID:IMSR_JAX:007909
B6.Cg-*Piezo1*$^{tm2.1Apat}$/J	The Jackson Laboratory	RRID:IMSR_JAX:029213
B6(SJL)-*Piezo2*$^{tm2.2Apat}$/J	The Jackson Laboratory	RRID:IMSR_JAX:027720
Oligonucleotides		
Piezo2	TaqMan assay	Mm01262433_m1
Trpv1	TaqMan assay	Mm01246300_m1
Gapdh	TaqMan assay	Mm99999915_g1
Software and algorithms		
Prism 6	GraphPad	https://www.graphpad.com/scientific-software/prism/
Illustrator CS6	Adobe	https://www.adobe.com/products/illustrator.html
EthoVision XT 13	Noldus	RRID: SCR_000441
Spike2 8.03	Cambridge Electronic Design Limited	RRID: SCR_000903
pClamp	Molecular Devices	RRID: SCR_011323
LabChart 7	ADInstruments	https://www.adinstruments.com/products/labchart
Other		
RNAscope probe: *Piezo2*	ACDBio	Cat#: 439971-C2